



# CALIFORNIA INSTITUTE OF TECHNOLOGY

EARTHQUAKE ENGINEERING RESEARCH LABORATORY

## AN ANALYSIS OF THE DYNAMIC CHARACTERISTICS OF A SUSPENSION BRIDGE BY AMBIENT VIBRATION MEASUREMENTS

BY

A. M. ABDEL-GHAFFAR AND G. W. HOUSNER

EERL 77-01

A REPORT ON RESEARCH CONDUCTED UNDER A  
GRANT FROM THE NATIONAL SCIENCE FOUNDATION

PASADENA, CALIFORNIA  
JANUARY 1977

CALIFORNIA INSTITUTE OF TECHNOLOGY  
EARTHQUAKE ENGINEERING RESEARCH LABORATORY

AN ANALYSIS OF THE DYNAMIC CHARACTERISTICS  
OF A SUSPENSION BRIDGE BY  
AMBIENT VIBRATION MEASUREMENTS

BY

A.M. Abdel-Ghaffar and G.W. Housner

EERL 77-01

A Report on Research Conducted under a Grant  
from the National Science Foundation

Pasadena, California

January, 1977

## ABSTRACT

Extensive experimental investigations were conducted on the Vincent-Thomas Suspension Bridge at Los Angeles Harbor to determine natural frequencies and mode shapes of vertical, torsional and lateral vibrations of the structure. These ambient vibration tests involved the simultaneous measurements of both vertical and lateral vibrational motions caused by traffic. Measurements were made at selected points on different cross sections of the stiffening structure. Comparison with previously computed mode shapes and frequencies shows good agreement with the experimental results, thus confirming both the accuracy of the experimental determination and the reliability of the method of computation.

## TABLE OF CONTENTS

<u>Title</u>	<u>Page</u>
Abstract	
Introduction	1
Types of Vibrational Motions of Suspension Bridges	3
The Vincent-Thomas Suspension Bridge	7
Description of the Instrumentation	12
Measuring Procedures	15
1. Installation	15
2. Operation	15
3. Recording	16
Data Processing and Analysis	23
1. Data Reduction	23
2. Natural Frequencies and Modes of Vibrations	24
Comparison of the Computed and Measured Natural Frequencies and Mode Shapes	35
1. Vertical Vibration	35
2. Torsional Vibration	48
3. Lateral Vibration	58
Damping	68
Conclusions	71
Acknowledgement	73
References	74
Appendix A	75

## INTRODUCTION

Performing tests on full-scale structures is the only sure way of assessing the reliability of the various assumptions employed in formulating mathematical or finite-element models of structures. It is also the most reliable way of determining the parameters of major interest in structural dynamics problems, such as natural frequencies, mode shapes and damping. Although many such experimental studies have been performed on buildings, only few measurements have been made on suspension bridges.<sup>1, 2, 5</sup> For these measurements, wind was the usual source of excitation, but high-speed vehicular traffic can also induce vibrations whose amplitudes, particularly in the higher modes, would be difficult to obtain by other means.

The improvements in modern motion-sensing instruments, measuring techniques and data processing and analysis have made it possible to acquire more extensive and accurate information about the dynamic properties of structures.

In 1971, McLamore, et. al.,<sup>1</sup> experimentally determined natural frequencies, damping and mode shapes of two American suspension bridges. Their objective was to determine vertical and torsional modes from recorded vertical motions in the frequency range 0.0 Hz - 1.0 Hz. Two torsional modes were identified, but no comparison was made with computed results.

In 1974-75, extensive repairs were planned to the deck of a Canadian suspension bridge, and in order to obtain guidance in

establishing the dynamic parameters for model tests and design calculations, measurements on the structure were carried out by Rainer and Selst.<sup>2</sup> The computed frequencies and mode shapes of torsional vibration predicted by a lumped mass, linear stiffness model differed substantially from the measured results.

Japan has obtained numerous experimental results<sup>7, 8, 9</sup> of static and dynamic responses of prototype suspension bridges, through a number of field tests and earthquake observations. The Kanmon Bridge,<sup>9</sup> completed in 1973, is the longest suspension bridge in Japan with a total length of 3,505 ft (1,068 m) and is one of those bridges on which comprehensive field measurements were taken.

In late 1975, a wide band of natural frequencies of the Vincent-Thomas Suspension Bridge (Los Angeles Harbor) were measured<sup>4, 5</sup> for vertical vibrations excited by traffic. These tests were performed in conjunction with a theoretical study in which a method of vibrational analysis of suspension bridges was developed. The results of the field measurements showed good agreement with the computed values. The experience gained in making these measurements was valuable in planning a subsequent more extensive program of measurements in which the shapes of modes of vibration were also obtained. The results of this second experimental program are reported here.

The purpose of making these field measurements and of formulating the method of dynamic analysis is to develop a reliable method for analyzing earthquake excited vibrations of suspension bridges.

## TYPES OF VIBRATIONAL MOTIONS OF SUSPENSION BRIDGES

The uncoupled vibrational modes of a suspension bridge may be classified as vertical, torsional and lateral, as shown in Fig. 1. In pure vertical modes, all points on a given cross section of the bridge move the same amount in only the vertical direction, and they remain in phase (Fig. 1-a). In pure torsional modes, each cross section of the bridge rotates about an axis which is parallel to the longitudinal axis of the bridge and which is in the same vertical plane as the centerline of the bridge. Corresponding points on opposite sides of the centerline of the roadway attain equal displacements, but in opposite directions (Fig. 1-b). In pure lateral motion, each cross section swings in a pendular fashion in its own vertical plane, and therefore there is upward movement of the cables and of the suspended structure incidental to their lateral movements, as shown in Fig. 1-c.

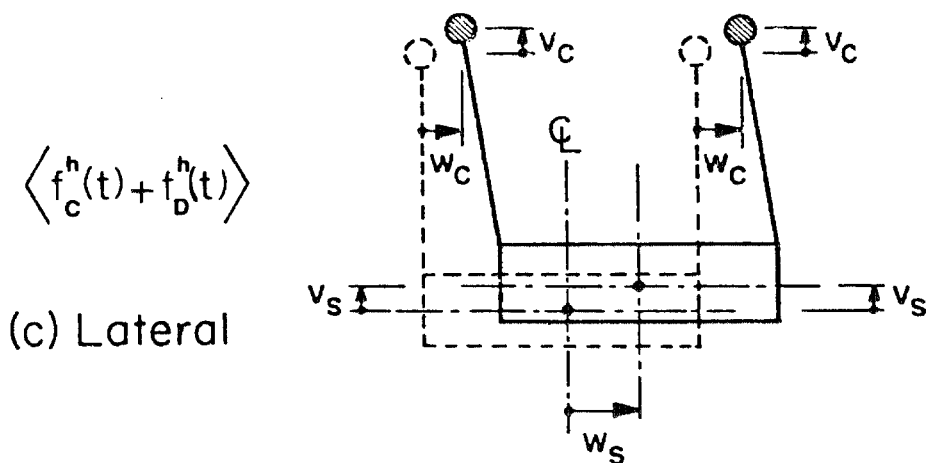
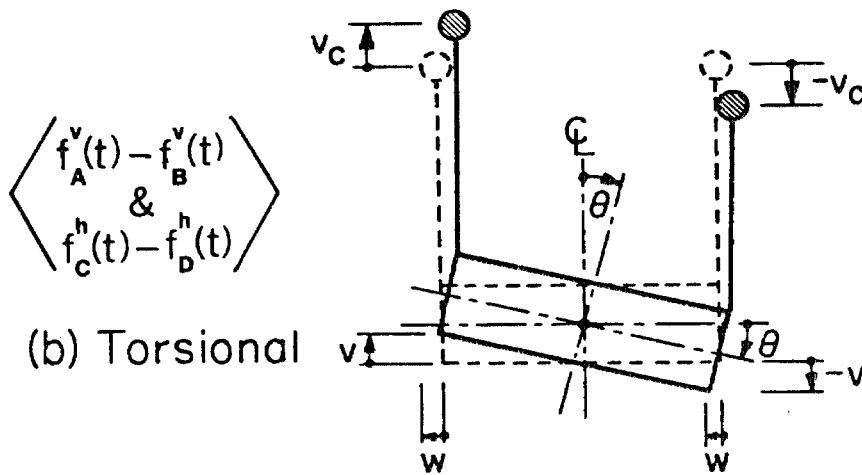
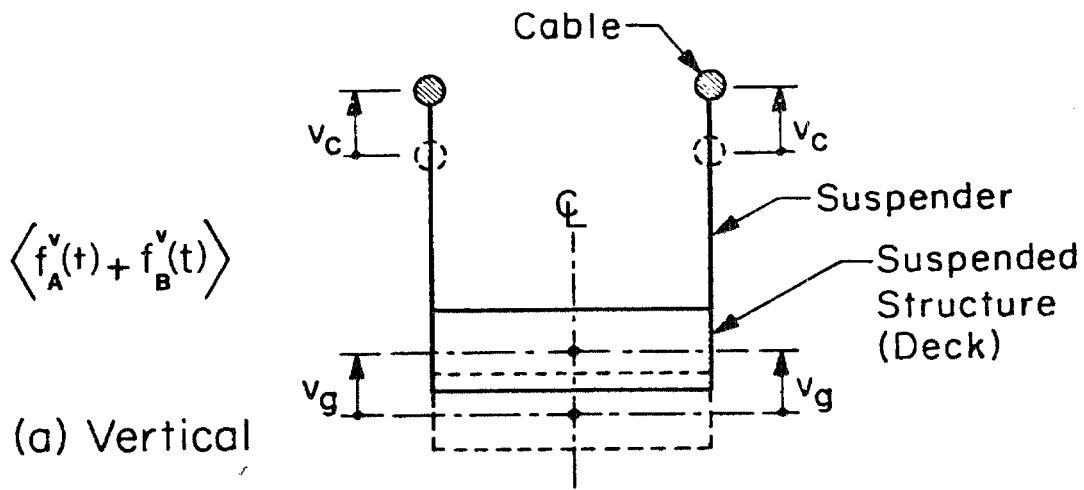
The measured vertical motions of the bridge (designated by  $f_A^V(t)$  and  $f_B^V(t)$  in Figs. 1 and 2) can be separated into the contributions of the vertical and the torsional modes by placing two vertically recording seismometers at the same cross section of the bridge, on the centerlines of the two stiffening trusses. Subtracting their outputs gives the torsional motion, and summing the outputs gives the vertical motion.

The measured lateral motion of the bridge (designated by  $f_C^h(t)$  and  $f_D^h(t)$  in Figs. 1 and 2) can be separated into the

contributions of the lateral and torsional modes by placing two horizontally recording seismometers at the same cross section, one on the top chord and the other directly below on the bottom chord of one stiffening truss. Summing the outputs gives information about the purely lateral vibration, and subtracting the outputs provides information on the purely torsional vibration.

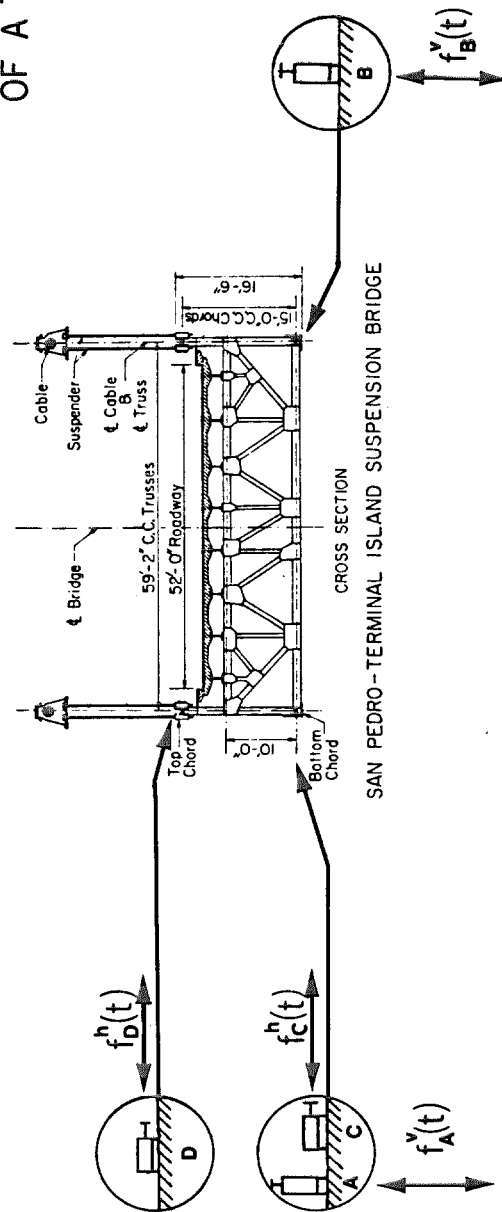
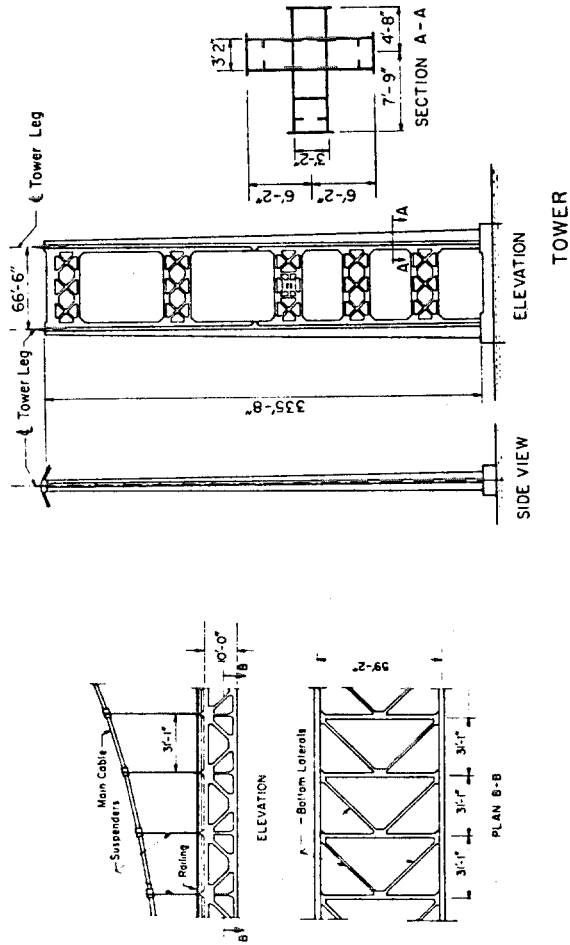
Figures 1 and 2 show, schematically, the basis for the measurements which was employed in the following experimental investigation.





TYPES OF VIBRATIONAL MOTION  
IN SUSPENSION BRIDGES

Fig. 1



## THE VINCENT-THOMAS SUSPENSION BRIDGE

The Vincent-Thomas Suspension Bridge (Fig. 3) was constructed in the early 1960's across the Main Channel of the Los Angeles Harbor from the city of San Pedro to Terminal Island. The bridge superstructure consists of a 1,500 ft suspended center span and two 506.5 ft suspended side spans, with a 52 ft wide four-lane roadway. The cables have a vertical sag of 150 ft at the center of the main span. Other dimensions of the structure are shown in Figs. 2 and 5. A detailed description of the bridge can be found in Ref. 3.

The suspended structure consists of two stiffening trusses, floor trussed beams and a lower chord wind bracing of K-truss type. The two stiffening trusses with the deck structure and lower chord bracing form a box-system having relatively high torsional rigidity. Transverse rolled-girders, 7 ft apart center to center, are supported by the transverse top chords of the floor truss. Lightweight concrete was utilized for the deck slabs.

The tower legs (Fig. 4) have cruciform cross sections made of four welded box sections, field bolted with one inch diameter high strength bolts. The cable consists of 4,028 cold drawn, galvanized, 6 gage steel wires providing 121.5 square inches of steel area. The ultimate strength of the wire was specified to be at least 225,000 psi thus providing a theoretical cable strength of 27,337 kips. The maximum design tension in the

cable at the towers was 9,620 kips for both gravity loading and live loads. This indicates a design factor of safety of about 3. The suspender cables are made of small diameter, high strength wires.



Fig. 3. General view of the Vincent-Thomas Suspension Bridge at Los Angeles Harbor (between the city of San Pedro and Terminal Island).

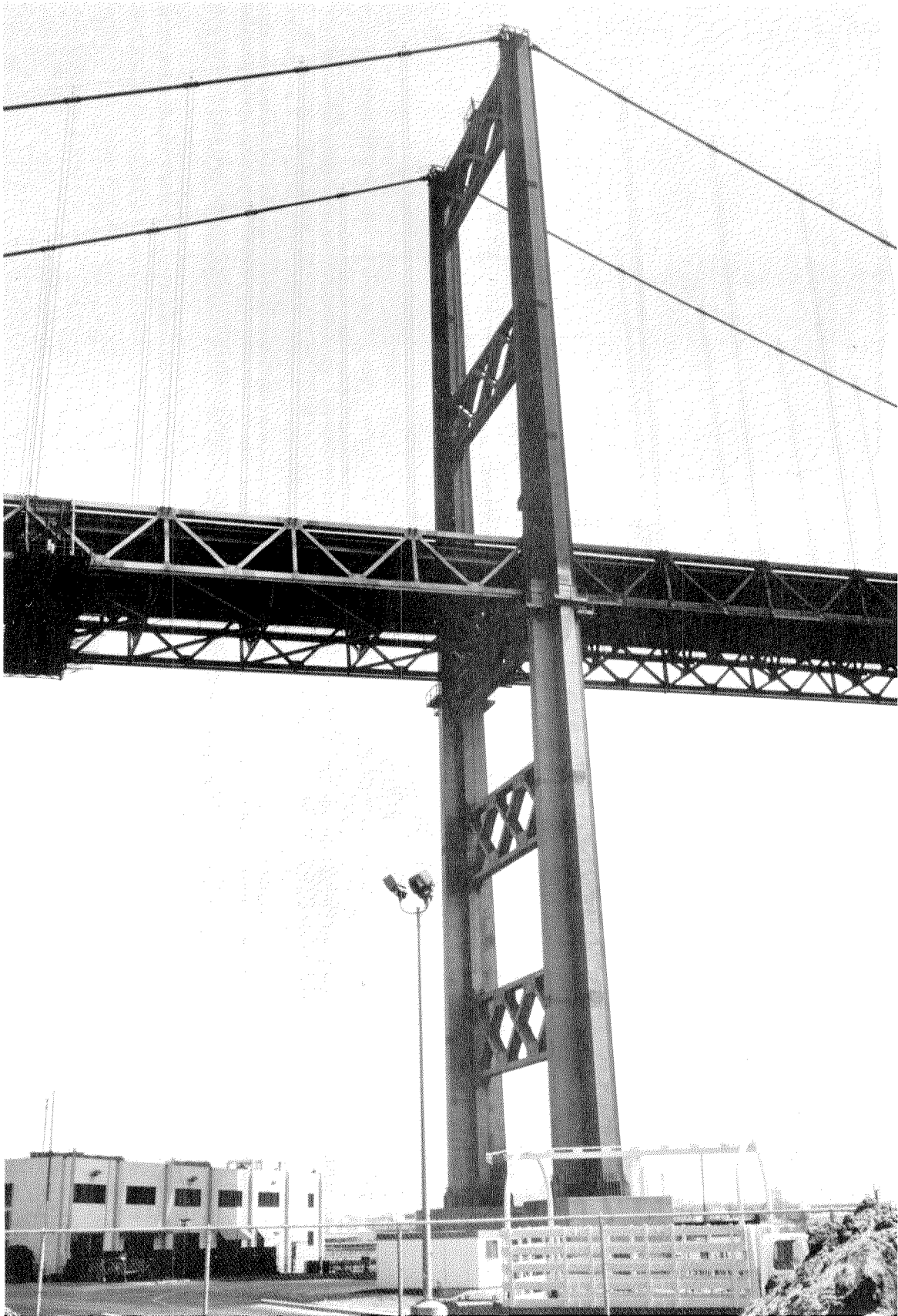
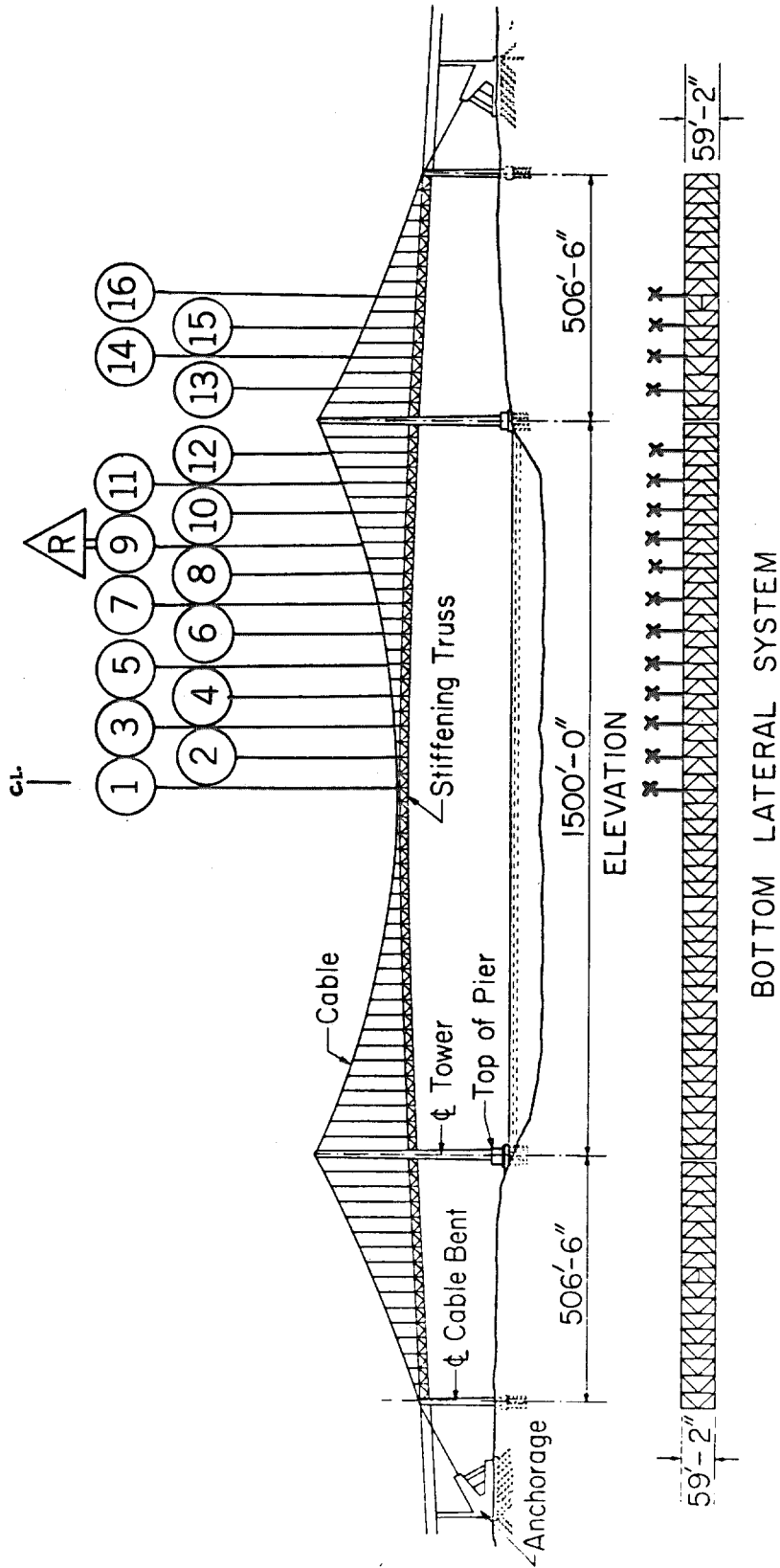


Fig. 4. General view showing one of the towers of the Vincent-Thomas Suspension Bridge and also showing the traveler.



SAN PEDRO-TERMINAL ISLAND SUSPENSION BRIDGE

MEASUREMENT STATIONS

Fig. 5

## DESCRIPTION OF THE INSTRUMENTATION

A short description is presented here of the measuring equipment used and of the deployment and orientation of the sensing instruments.

### 1 - Kinometrics SS-1 Ranger Seismometer

The SS-1 Ranger seismometer is a short period, velocity type transducer with a natural period close to one second. A more detailed description is given in Refs. 3 and 6. The traffic excited motion of the bridge was measured by means of eight seismometers mounted at various locations on the bridge. Four seismometers were used to simultaneously measure vertical and lateral motions of each cross section or station, as indicated in Figs. 1, 2 and 5. Seismometers A and B (Fig. 2) were used to measure vertical motion at the bottom chords of the two stiffening trusses, while seismometers C and D were used to measure lateral motion at the top and bottom chords of one stiffening truss. This group of four transducers was moved from point to point to measure vertical and lateral motions of the bridge (see Fig. 5). Four reference seismometers (RA, RB, RC and RD) were located at the cross section designated by R, in Fig. 5, where they remained throughout all the tests. They were oriented in directions corresponding to seismometers A, B, C and D. The reference cross section was chosen so as to obtain as many mode shapes as possible in the frequency range 0.0 Hz - 3.0 Hz; i.e., it was placed so as not to be at a node of a mode. Measurements were made at 16 different



cross sections, and each time simultaneous measurements were made at the reference cross section. In this way the amplitudes at the measured cross section were determined relative to the amplitudes at the reference cross section.

## 2 - Kinemetrics SC-1 Signal Conditioner

Two four-channel signal conditioners were used during the tests to amplify, filter and simultaneously control the eight outputs from the seismometers. Each channel of the signal conditioners is adjustable to provide displacement, velocity or acceleration outputs. The signal conditioners also provide optional low-pass filters which are continuously adjustable between 1 and 100 Hz. During the ambient tests, it was decided to filter out all frequencies higher than 3 Hz. The power for the two signal conditioners was provided by an A.C. power source in the tower leg.

## 3 - Hewlett-Packard 3960A Instrumentation Tape Recorder

During the tests, the amplified and filtered signals were recorded on two four-channel HP tape recorders. The electrical outputs of these recorders can be digitized for computer processing by means of an analog-digital converter.

## 4 - Hewlett-Packard 7418A Oscillograph Recorder

The measurements taken during the ambient tests were monitored on an eight-channel HP Oscillograph Recorder. This also enabled an immediate visual inspection of the vibrational motion during each measurement.

5 - Kinematics DDS-1103 Electronic Analog-Digital Converter

The recorded tapes were taken to the Caltech dynamics laboratory where the recorded analog signals were digitized using an analog-to-digital converter.

## MEASURING PROCEDURES

### 1. Installation

The recording instruments, consisting of the signal conditioners, the tape recorders and the oscillograph recorder, were placed in the traffic lane close to the tower leg as shown in Figs. 6, 7 and 8. As an aid to the testing, this lane was blocked by the Bridge Authority during the time that measurements were taken.

The eight seismometers were first placed at the reference station (cross section R). They were connected to the recording instruments by means of eight electrical cables. Six cables were run along the inspection walk underneath the bridge deck (Fig. 10) leading to the traveler which was used to move from station to station (Figs. 4, 10 and 11). The traveler was also first located at station R. Two cables were run along the sidewalk leading to the reference station (Fig. 6).

### 2. Operation

Since the natural frequencies of the seismometers are in the range of the measured frequencies and since the natural period and damping is not identical for each instrument, the transfer functions of the instruments are not identical. Consequently, relative calibration must be made at all the frequencies of interest. To achieve this, the instruments were aligned side by side at one location (station R) with four seismometers (A, B, RA and RB) in the vertical direction, and the other four seismometers (C, D, RC and RD) in the

lateral direction. The eight seismometers were adjusted in preparation for recording at their location. The recording instruments were also adjusted in order to make sure that the signals were within the limits of operation of both the tape recorders and the oscillograph recorder.

### 3. Recording

The recording began after several minutes of visually monitoring the vibrations (by the oscillograph recorder), during which the fine adjustments were made. Vertical as well as lateral vibrational motions were recorded for about ten minutes during the first calibration run. Then seismometers A, B, C and D were mounted on the cross section, as shown in Fig. 2, with each seismometer placed at the same location as its reference; for example, seismometer A with RA and C with RC, etc. During the second run, seismometers RA, RB, RC and RD remained at their original locations (as throughout all the tests) while seismometers A, B, C and D were moved to station 1 (mid-point cross section of the center span) by using the traveler. The adjustment and recording procedures were repeated. The above procedures were repeated for stations 2 through 16; Figs. 9 and 11 show seismometers D, A and C in their locations during the seventeen runs of testing. Each record or test is indicated by the number of the station at which seismometers A, B, C and D were placed, followed by the "name" of the seismometer, e.g., 6-A, 6-RA, etc.

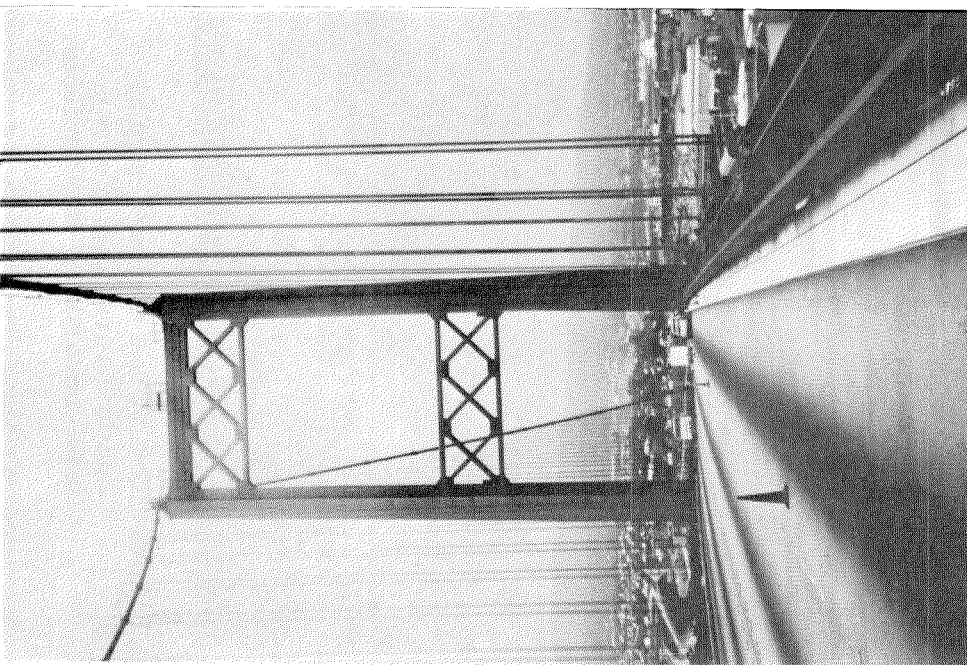


Fig. 6. General view of the Vincent-Thomas Bridge showing the location of the recording instruments (close to the tower leg) and the cables stretched along the sidewalk.

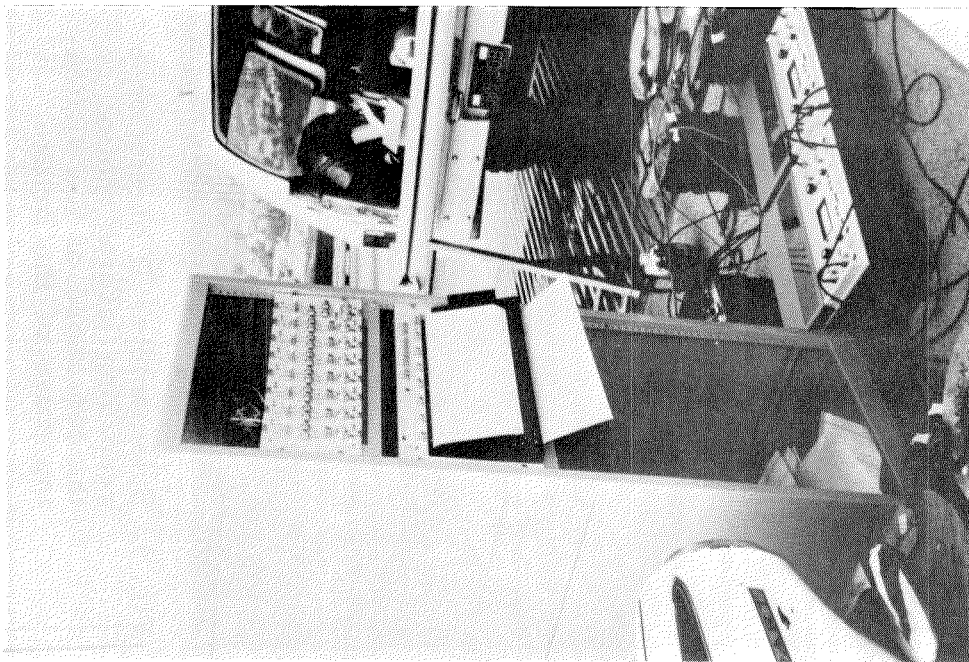


Fig. 7. The 8-channel oscillograph recorder and the two 4-channel instrumentation tape recorders used for the ambient tests.

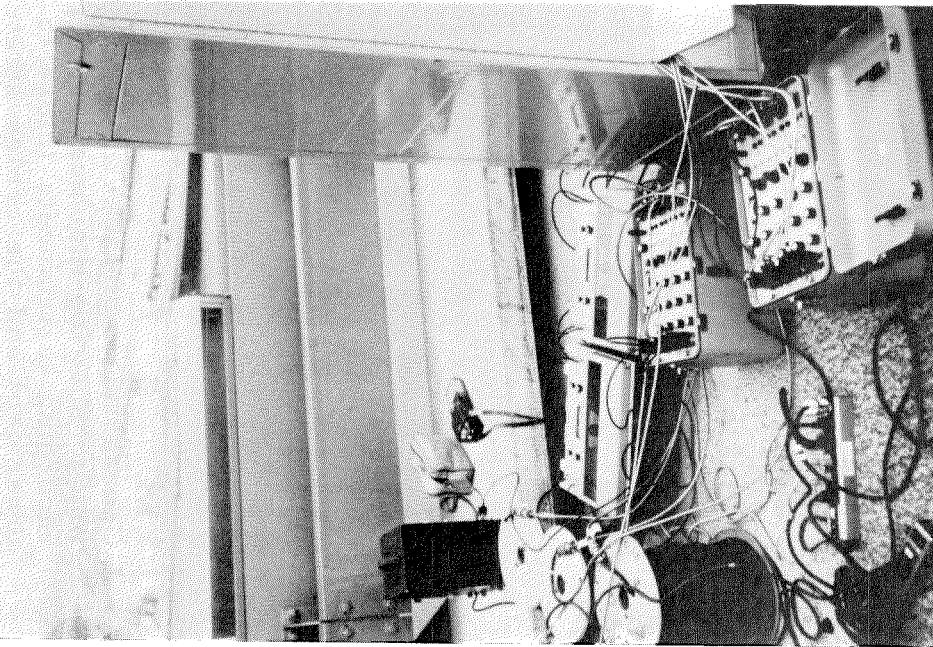


Fig. 8. The two 4-channel signal conditioners and the two tape recorders in the field.

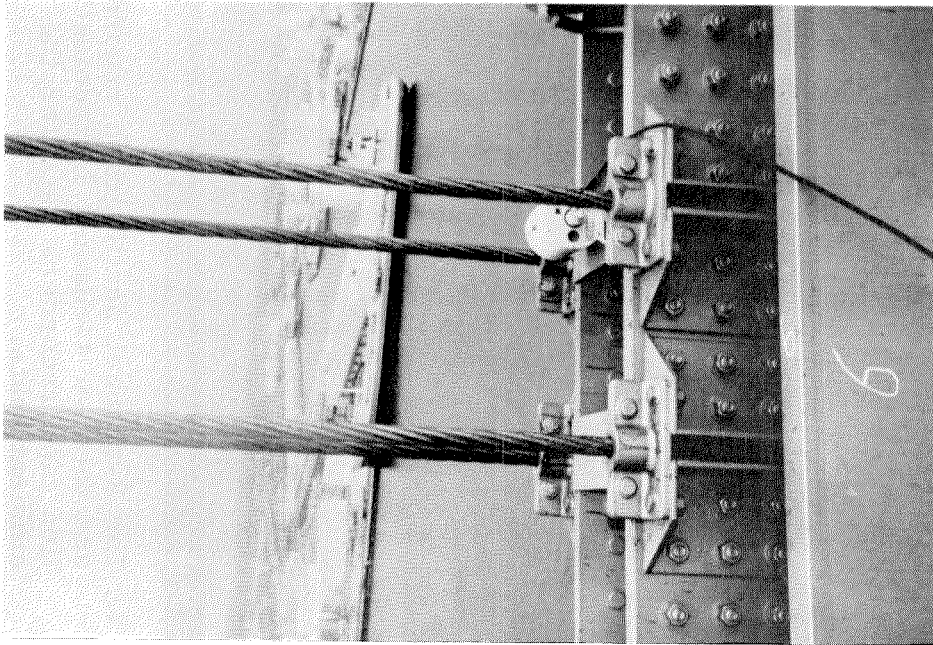


Fig. 9. Seismometer D at station 6 recording lateral motion of the top chord of the stiffening truss of the bridge.

As mentioned previously, each signal conditioner provides independent integration and differentiation; consequently, output signals proportional to displacement and acceleration were available. In all tests, the velocity circuits of the two signal conditioners were used to measure the motion due to higher modes since these enhance the higher frequencies of the motion. Sample traces from the oscillograph recorder made during the tests at station 5 are shown in Fig. 12.

There was very little wind during the two days of tests so that the vibrations of the bridge were mainly caused by vehicular traffic.

All of the instruments functioned satisfactorily throughout the tests except seismometers RA and RC which behaved erratically during most of the tests. Because it was extremely difficult to reach and check these two seismometers during the tests (except tests 1 and 2), it was decided to depend completely on seismometers RB and RD as references for the vertical and lateral motions, respectively.

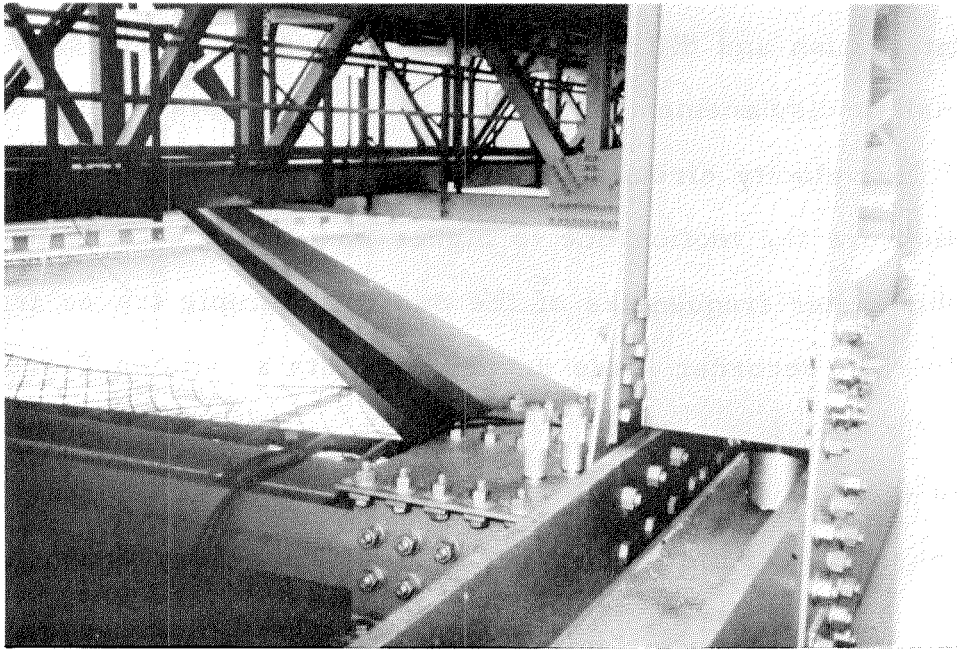


Fig. 10. General view showing the inspection walk, the traveler and the lower wind bracing members.

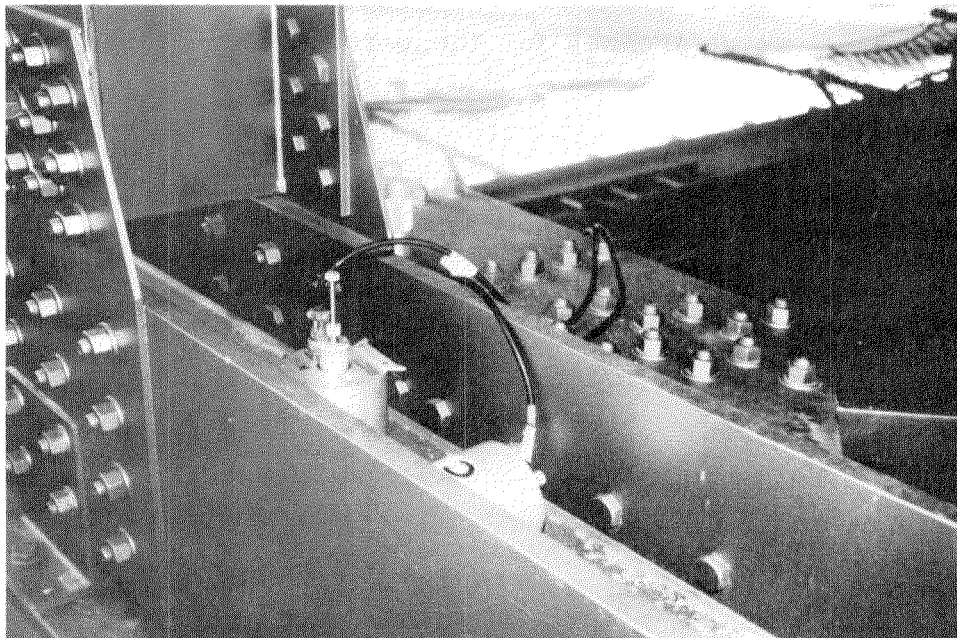


Fig. 11. The two seismometers A and C recording the vertical and lateral motions, respectively, of the bottom chord of the stiffening truss of the bridge.



Table 1

Sequence of Tests to Determine Mode-shapes of the  
San Pedro-Terminal Island Suspension Bridge  
(Instrument Locations)

No.	Reference Location (Station Number)				Variable Location (Station Number)			
	Vertical Motion		Lateral Motion		Vertical Motion		Lateral Motion	
	Seismometer No.				Seismometer No.			
	RA	RB	RC	RD	A	B	C	D
1*	9	9	9	9	9	9	9	9
2**	9	9	9	9	9	9	9	9
3	9	9	9	9	1	1	1	1
4	9	9	9	9	2	2	2	2
5	9	9	9	9	3	3	3	3
6	9	9	9	9	4	4	4	4
7	9	9	9	9	5	5	5	5
8	9	9	9	9	6	6	6	6
9	9	9	9	9	7	7	7	7
10	9	9	9	9	8	8	8	8
11	9	9	9	9	10	10	10	10
12	9	9	9	9	11	11	11	11
13	9	9	9	9	12	12	12	12
14	9	9	9	9	13	13	13	13
15	9	9	9	9	14	14	14	14
16	9	9	9	9	15	15	15	15
17	9	9	9	9	16	16	16	16

\*All 8 seismometers were placed at the same location (point A)  
at station No. 9.

\*\*Each seismometer was placed at the same location as its  
reference. (e. g., A with RA and C with RC) at station No. 9.

Note: Each test is designated by the station no. of the location  
and by the seismometer no. (e. g., 5-A, 5-B, 5-RA, 5-RB).

A



RA



B



RB



C



RC



D



Fig. 12. Sample traces from the oscillograph recorder made simultaneously during ambient vibration tests of cross section no. 5 of the Vincent-Thomas suspension bridge.

## DATA PROCESSING AND ANALYSIS

### 1. Data Reduction

The recorded data were converted to digital format on magnetic tape compatible with the digital computer to be used. The digitization was at a rate of 30 equally spaced points per second which resulted in a Nyquist frequency of 15 Hz; this is well above all the frequencies being considered (3 Hz). For each record, 8,192 data points were generated corresponding to 273.07 seconds.

A Fast Fourier Transform (FFT) was then computed for the 8,192 points of each seismometer record resulting in 4,097 spectral ordinates and phase angles. The frequency resolution was  $15/4,097$ , or about 0.0037 Hz, which is a favorably high resolution. The spectra were next smoothed with only one pass of a Hanning Window ( $\frac{1}{4}, \frac{1}{2}, \frac{1}{4}$  weights). This smoothing of the spectra facilitates the selection of the natural frequencies and, consequently, the identification of the associated modes of vibration.

Care was taken not to obliterate two peaks when two modes were closely spaced in the frequency domain. One smoothing pass was made due to the following:

1. When an attempt to use the unsmoothed spectra to recover modes and frequencies of vibrations was made, it was sometimes difficult to make accurate estimates of the frequencies and associated modes due to special overlap in the peak areas and due to multiple peaks centered in a very narrow band of frequencies.

2. Though the vibration of the bridge when vehicles are passing is presumably a non-stationary random process, the spectral peaks do not seem to be at exactly the same frequencies for different stations. One possible explanation for this phenomenon is that several modes of vibration were excited in varying amounts from one test (or station) to the other because of the variable traffic density and different speed, weight and direction of the vehicles. Thus, for better representation of the frequency content of the response, smoothing the spectrum was necessary.

The distribution of the discrete Fourier amplitude spectra versus the discrete frequencies was then plotted for the  $8 \times 17 = 136$  recorded signals, and the natural frequencies of vibrations were picked to correspond with the points about which the data clustered. Since Fourier amplitude spectra give only the modulus of the amplitude, phase spectra were used to determine the in-phase or  $180^\circ$  out-of-phase sign of the modal amplitudes. The Fourier amplitude spectra of the recorded vertical and lateral motions at stations 5 and 7 are shown in Figs. 13 through 16.

## 2. Natural Frequencies and Modes of Vibrations

The procedure for determining mode shapes was to divide the smoothed spectral amplitude of the response at a given station by the smoothed spectral amplitude of the simultaneously recorded response at the reference station. In this way, an amplitude proportional to

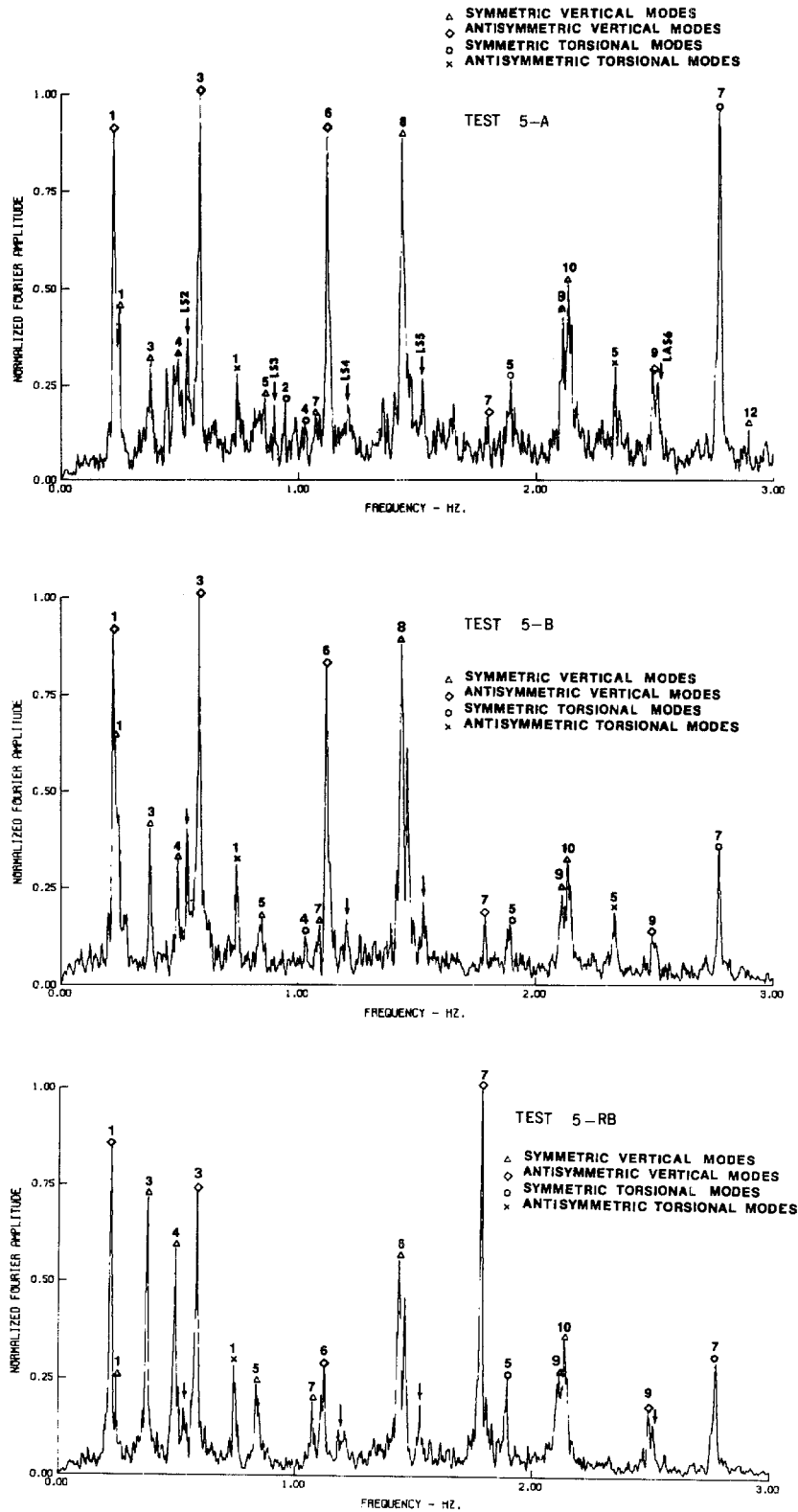


Fig. 13. Fourier amplitude spectra of the velocity proportional response of the vertical motions recorded, simultaneously, at station 5 and the reference station.

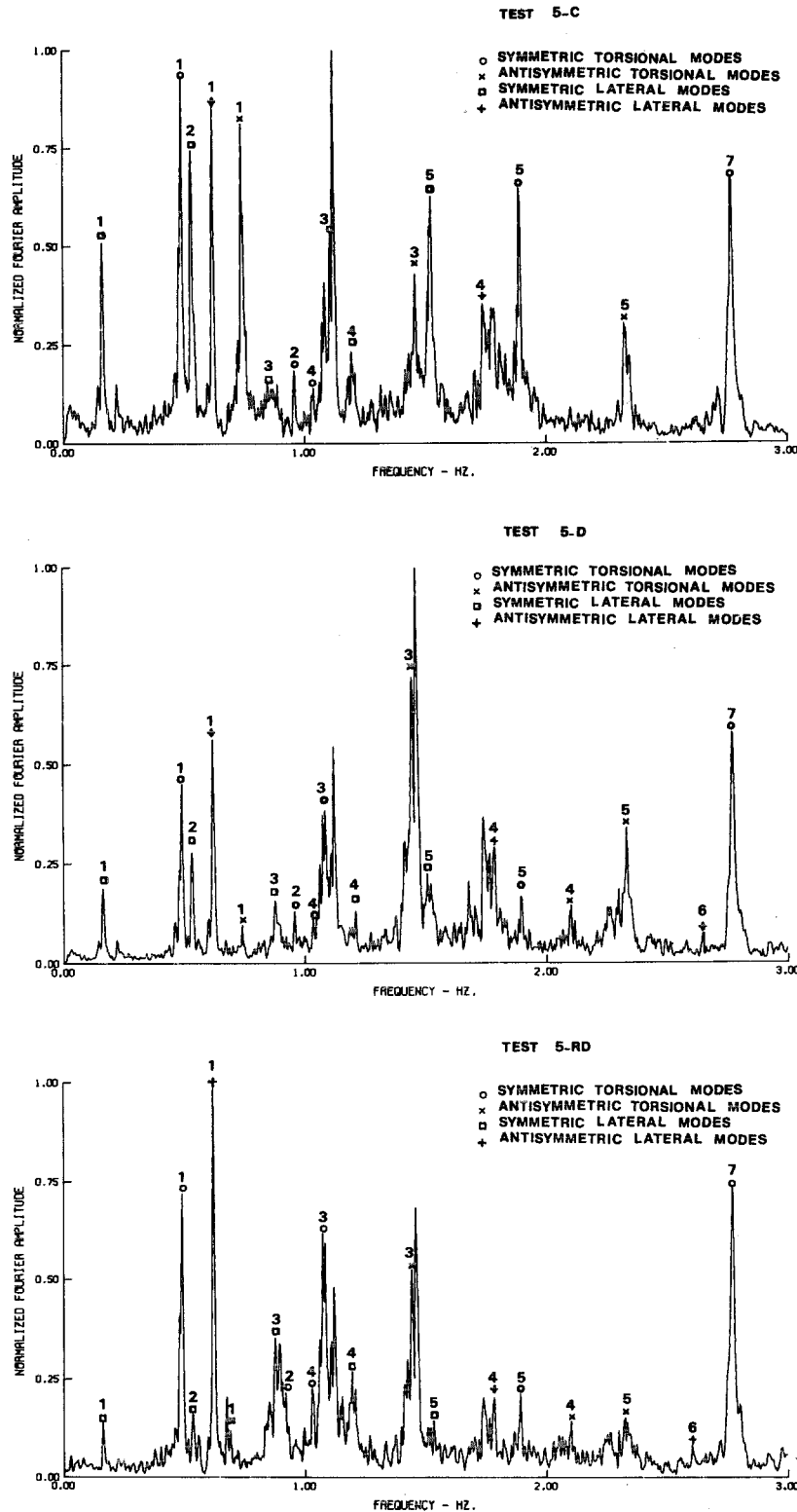


Fig. 14. Fourier amplitude spectra of the velocity proportional response of the lateral motions recorded, simultaneously, at station 5 and at the reference station.

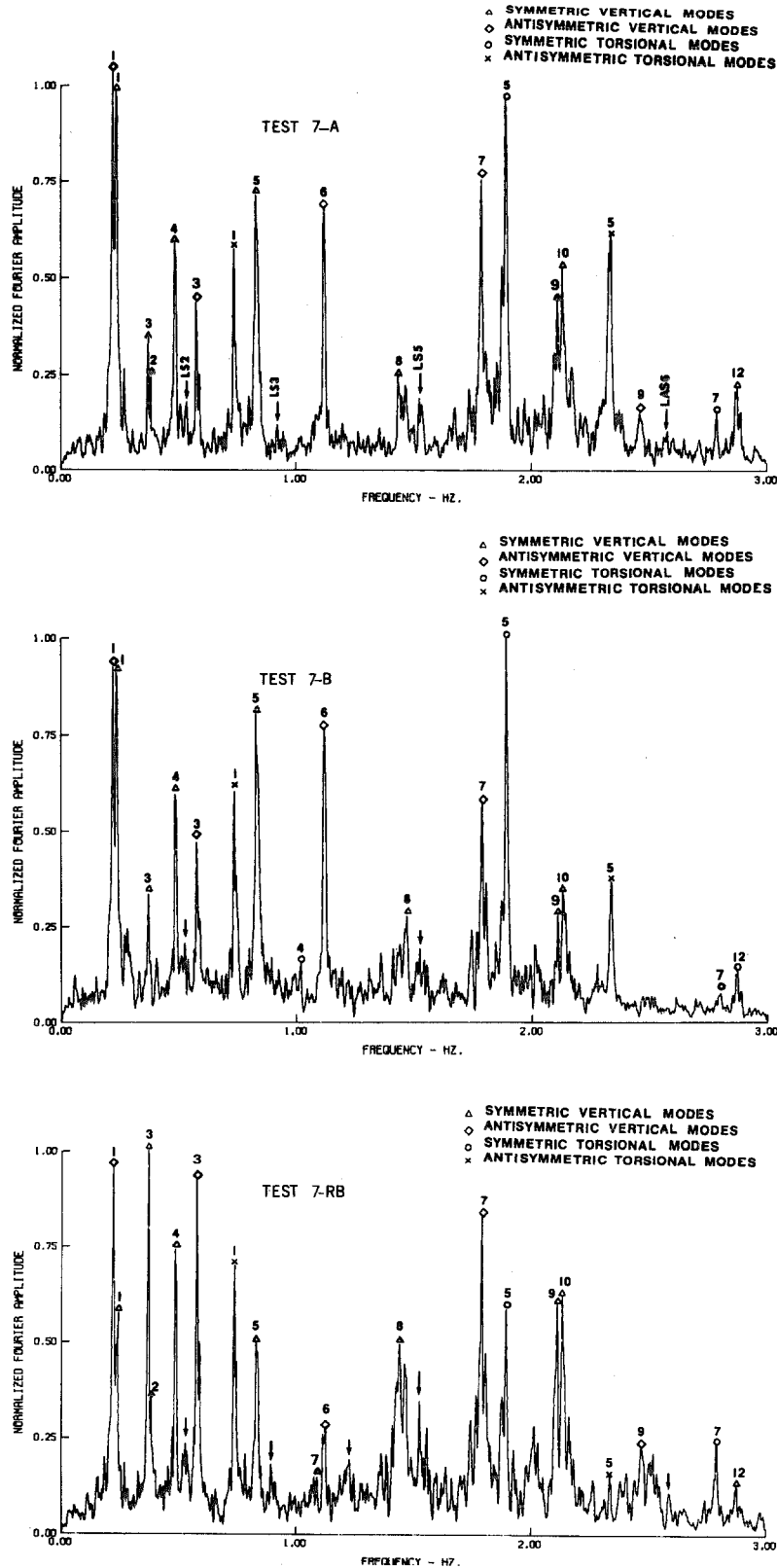


Fig. 15. Fourier amplitude spectra of the velocity proportional response of the vertical motions recorded, simultaneously, at station 7 and at the reference station.

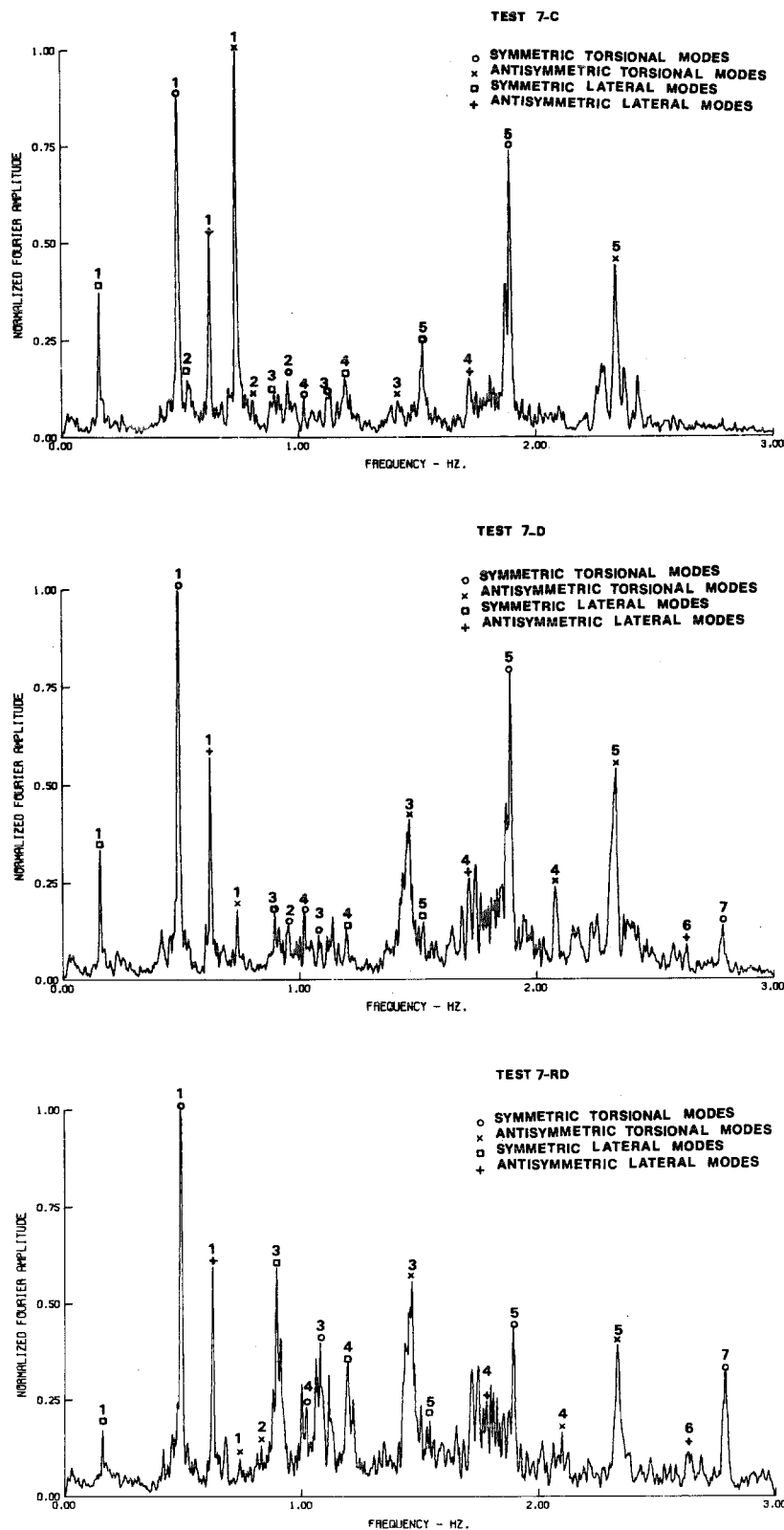


Fig. 16. Fourier amplitude spectra of the velocity proportional response of the lateral motions recorded, simultaneously, at station 7 and at the reference station.



the mode shape amplitude at that station is obtained for a given frequency of vibration, and as mentioned before, relative calibration was made at all the frequencies of interest. Repeating this procedure for stations 1 through 16, the mode shapes were determined. The phase of the response was compared to that of the reference instrument to determine the signs of the modal displacements.

In addition, the following procedures were used in identifying different mode shapes and their associated frequencies:

1. As a preliminary step, the mode shapes were identified from the individual records, i.e., without summing or subtracting these records. The good separation of the spectral peaks, as shown in Figs. 13 through 16, as well as the availability of the computed mode shapes and frequencies (Ref. 3) and also the results of previous experimental work (Ref. 5), all helped in this step. In case of spectral overlap in the peak areas or multiple peaks, all the modes corresponding to the discrete frequencies which covered this spectral peak area were plotted. It was easy to decide whether this spectral peak area contained one or more modes by studying the trend of all the plotted modes.
2. Mode shapes were determined by adding the vertical (or lateral) response of seismometers A and B (or C and D) to enhance vertical (or lateral) vibration; the

signals were subtracted to emphasize torsional motions in both vertical and lateral directions. During steps 1 and 2 the following details were observed.

- i - Two vertical (lateral) modes or two torsional modes or a vertical (lateral) and a torsional mode were sometimes at nearly the same frequency, and separating them was difficult. High frequency resolution was helpful, but in some cases it was still extremely difficult to separate the modes. In other cases, the two close modes were somewhat distinct.
- ii - The frequencies corresponding to the spectral peaks were determined on a statistical basis. As mentioned previously, the spectral peaks were not always at precisely the same frequencies. Also, if two modes are closely spaced in the frequency domain, superposition of their Fourier amplitude spectra might lead to a shifting of the apparent peak. For this reason, it may be erroneous to pick the frequencies from one or two spectrum peaks only.
- iii - Mode shapes resulting from either recorded vertical or lateral vibrations were determined by averaging the modal amplitudes resulting from individual seismometer records and the modal

amplitudes resulting from summing or subtracting the records. In each case, the mode was determined as the average of the modal amplitudes corresponding to three adjacent discrete frequencies, i.e., at the natural frequency in question, plus or minus 0.0037 Hz (the frequency resolution interval).

iv - For the torsional modes, the modal amplitudes resulting from both recorded vertical and lateral motions were plotted. Generally, all the torsional modes were recovered from recorded lateral motion. Only 6 torsional modes out of 11 were recovered from vertical motion. One possible explanation for this is that some vertical and torsional modes are very closely spaced, and the exact separation of these modes is not possible from this set of data, even by subtracting the two vertical records of seismometers A and B. Actually, the recorded vertical motion at those frequencies is dominated by the vertical modes rather than by the torsional modes, and in some instances, the vertical component of torsional motion was so small as to be unclear. Thus, the torsional modes were not as clear and distinct as the vertical modes. The following table contains those identified modes whose frequencies of vibration are close together.

Table 2

Torsional Modes (from Lateral Motion)		Vertical Modes (from Vertical Motion)	
Mode Shape	Measured Frequency (Hz.)	Mode Shape	Measured Frequency (Hz.)
T-S-1	0.494	V-S-4	0.491
T-AS-2	0.809	V-S-5	0.835
T-S-3	1.069	V-S-7	1.078
T-AS-3	1.425	V-S-8	1.450
T-AS-4	2.109	V-S-9	2.076

- v - As expected from the theoretical analyses (Ref. 3), there is upward vibrational motion of the suspended structure incidental to its lateral movements. This is seen from the peaks indicated by the arrows in the Fourier spectra of the recorded vertical motion (see Figs. 13 and 15).
- vi - In plotting the mode shapes of different vibrations, the symmetry of the structure has been used. However, the stations where measurements were actually taken are indicated by the mark x on the centerline of the stiffening structure. For a statistically more precise determination of modal amplitudes and for better resolution of the mode shapes, more experimental points would be required. This was impractical due to the limitation of both the measuring equipment and the time allowed for testing.
- vii - Finally, although the modes are determined by only a few discrete points, a linear interpolation through these points is made to approximate the continuous mode shapes.

Figure 17 summarizes the instrumentation used in the tests, the measuring procedures, the data processing and the experimental set-up of the ambient vibration tests on the Vincent-Thomas Suspension Bridge.

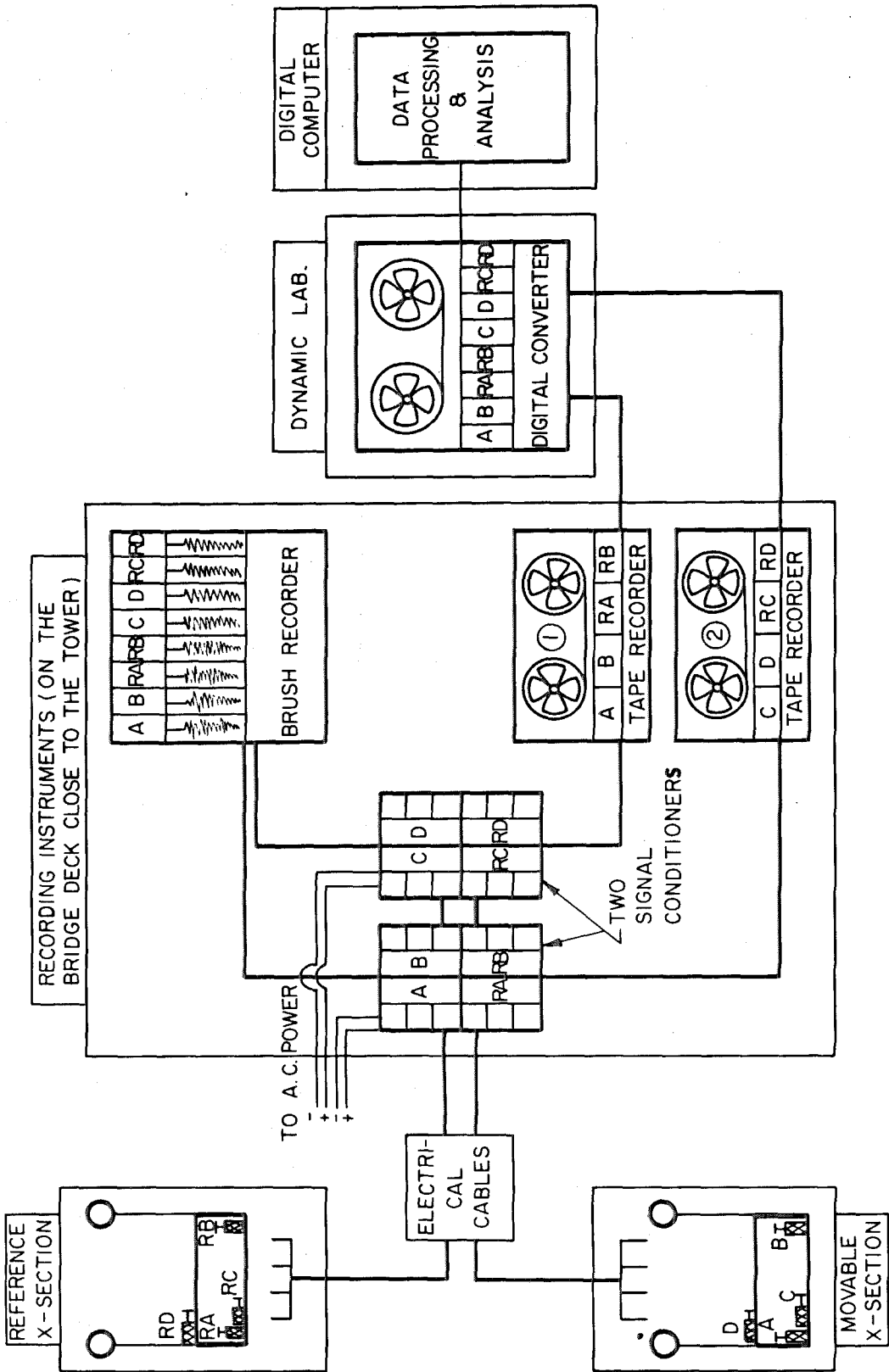


Fig. 17. Schematic diagram showing the experimental set-up and the data processing of the ambient vibration tests of Vincent-Thomas Bridge.

## COMPARISON OF THE COMPUTED AND MEASURED NATURAL FREQUENCIES AND MODE SHAPES

The mode shapes and natural frequencies determined by the ambient tests of the Vincent-Thomas Suspension Bridge are compared in Figs. 18 through 25 to those obtained by finite-element analysis (Ref. 3). Certain similarities and differences between the measured and the computed natural frequencies and mode shapes are apparent and they are discussed in the following paragraphs.

### 1 - Vertical Vibration

As indicated in Figs. 18 and 25, in the first eight symmetric mode shapes (except the 6th tower-mode) there is generally an excellent agreement between the measured and computed mode shapes and their associated natural frequencies. However, mode V-S-7 shows some coupled vibrational motion of the center and the side spans. The slightly higher calculated natural frequencies, for modes V-S-9, V-S-10 and V-S-12, resulting from the finite-element model may in part be due to the necessary simplifications in the theory, such as neglecting rotatory inertia and shear deformation and also confining the effect of additional cable tension to only the first few modes.

In the linearized problem of suspension bridge vibrations, the role played by the extensibility of the cable is confined to only the first few symmetric modes of vibration where the interaction between

the side and center spans exists. Thus, the agreement between the computations and the measurements for the higher mode shapes can be expected to become less satisfactory.

The natural frequencies and mode shapes for the antisymmetric vertical modes (Figs. 19 and 25) also show good agreement between the calculations and the measurements, despite the disappearance of the measured antisymmetric modes V-AS-2 and V-AS-8 (first and third side span modes). The computed second symmetric mode, V-S-2 (0.348 Hz) and the computed second antisymmetric mode, V-AS-2 (0.346 Hz), are actually identical except for the fact that in the symmetric case the two side spans are moving in-phase while in the antisymmetric case they are moving  $180^\circ$  out-of-phase. This, coupled with the fact that measurements were taken only on half of the bridge, suggests that the measured second symmetric mode of Fig. 18-a could be representative of the second antisymmetric mode shape. The same argument is also true for the computed ninth symmetric mode, V-S-9 (2.340 Hz) and the computed eighth antisymmetric mode, V-AS-8 (2.338 Hz).

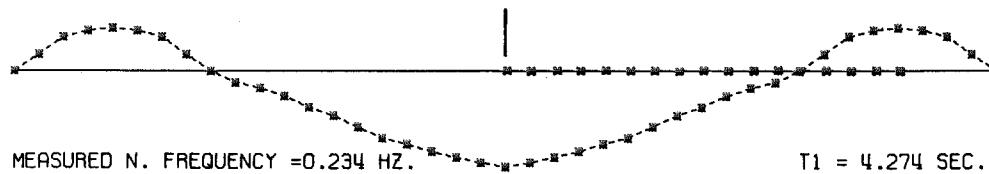
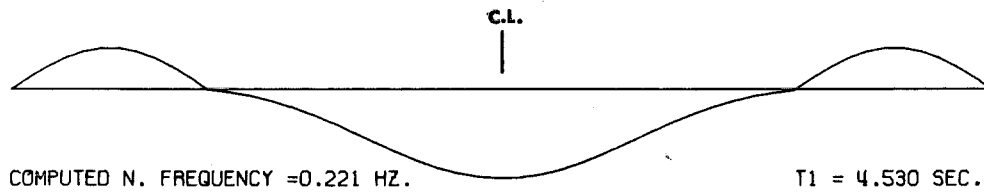
Also in the linearized problem of suspension bridge vibrations, the antisymmetric deflections of the cable and the stiffening structures cause no additional cable tension because the downward movement on one side of the centerline of the center span tends to increase the cable length, while at the same time the upward movement on the other side of the center span tends to reduce cable length, and the two effects balance each other. In consequence



of the lack of additional cable tension, there is no interaction between the center span and the side spans; i. e., two types of independent vibration are possible. However, the interaction between the side and the center spans is still found in the experimental results even in the higher modes, as shown in Figs. 19-b and 19-c.

Tables 3 and 4 summarize the comparison between the measurements and the computations of the vertical modes of vibration for both the symmetric and antisymmetric cases.

SAN PEDRO-TERMINAL ISLAND SUSPENSION BRIDGE  
AMBIENT VIBRATION TESTS  
SYMMETRIC VERTICAL VIBRATION



SAN PEDRO-TERMINAL ISLAND SUSPENSION BRIDGE  
AMBIENT VIBRATION TESTS  
SYMMETRIC VERTICAL VIBRATION

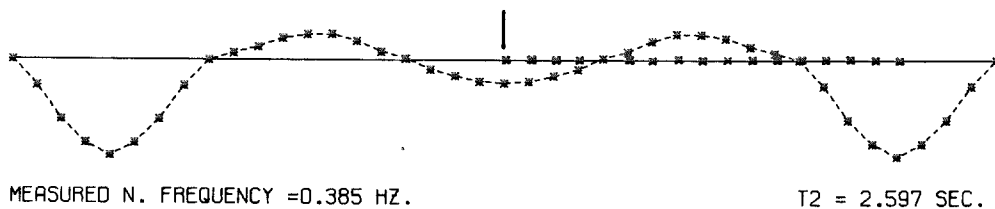
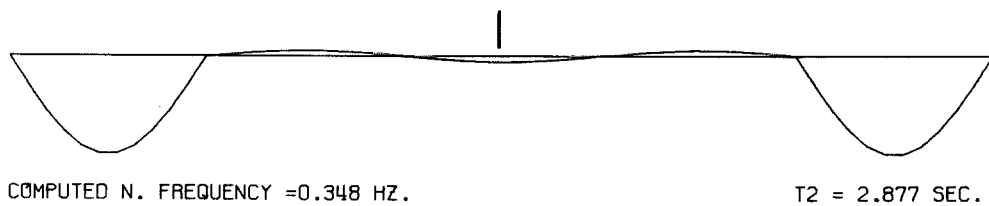
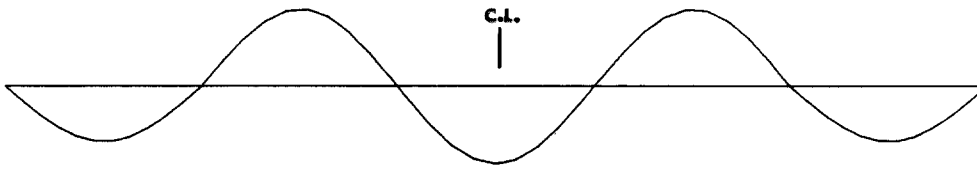


Fig. 18-a. Comparison between computed and measured natural frequencies and mode shapes of symmetric vertical vibration of the Vincent-Thomas Bridge.

SAN PEDRO-TERMINAL ISLAND SUSPENSION BRIDGE  
AMBIENT VIBRATION TESTS  
SYMMETRIC VERTICAL VIBRATION



COMPUTED N. FREQUENCY = 0.348 HZ.

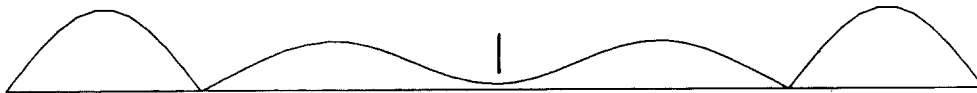
T3 = 2.870 SEC.



MEASURED N. FREQUENCY = 0.366 HZ.

T3 = 2.732 SEC.

SAN PEDRO-TERMINAL ISLAND SUSPENSION BRIDGE  
AMBIENT VIBRATION TESTS  
SYMMETRIC VERTICAL VIBRATION



COMPUTED N. FREQUENCY = 0.459 HZ.

T4 = 2.180 SEC.

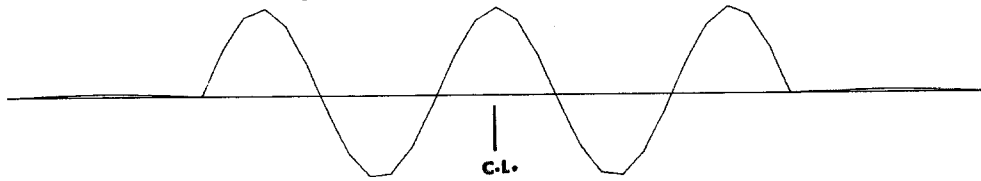


MEASURED N. FREQUENCY = 0.487 HZ.

T4 = 2.053 SEC.

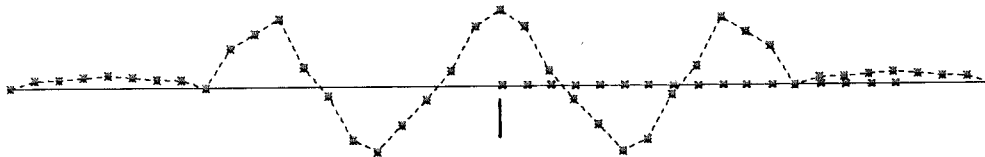
Fig. 18-b

SAN PEDRO-TERMINAL ISLAND SUSPENSION BRIDGE  
AMBIENT VIBRATION TESTS  
SYMMETRIC VERTICAL VIBRATION



COMPUTED N. FREQUENCY = 0.803 HZ.

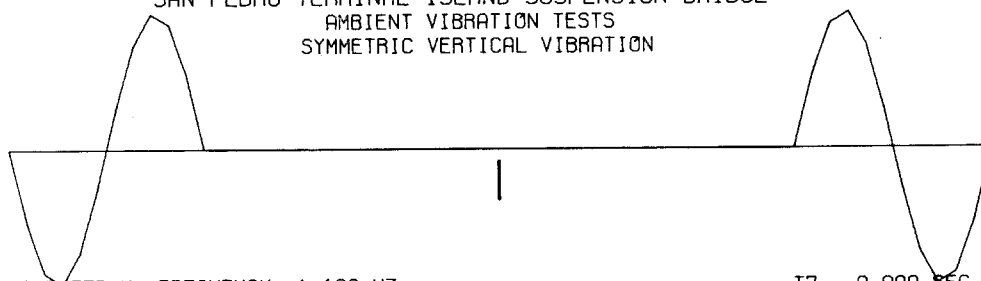
T5 = 1.245 SEC.



MEASURED N. FREQUENCY = 0.835 HZ.

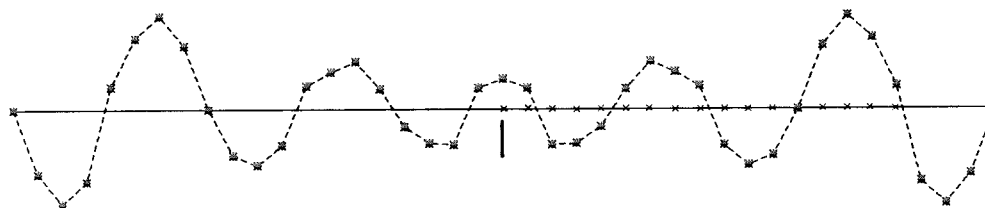
T5 = 1.198 SEC.

SAN PEDRO-TERMINAL ISLAND SUSPENSION BRIDGE  
AMBIENT VIBRATION TESTS  
SYMMETRIC VERTICAL VIBRATION



COMPUTED N. FREQUENCY = 1.100 HZ.

T7 = 0.909 SEC.

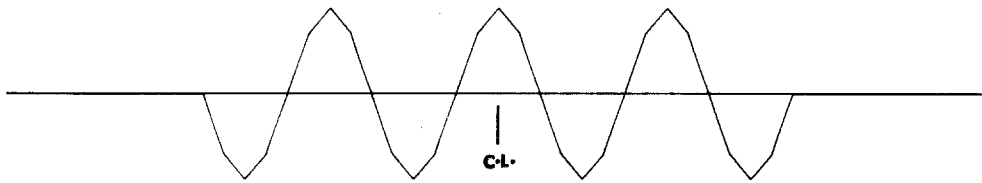


MEASURED N. FREQUENCY = 1.077 HZ.

T7 = 0.929 SEC.

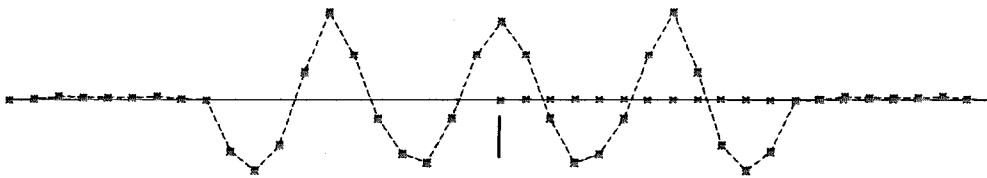
Fig. 18-c

SAN PEDRO-TERMINAL ISLAND SUSPENSION BRIDGE  
AMBIENT VIBRATION TESTS  
SYMMETRIC VERTICAL VIBRATION



COMPUTED N. FREQUENCY = 1.467 HZ.

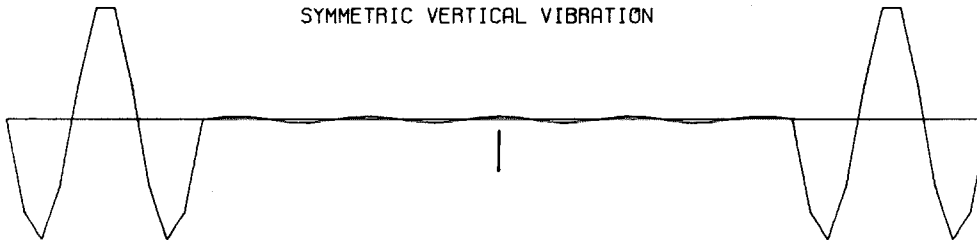
T8 = 0.682 SEC.



MEASURED N. FREQUENCY = 1.450 HZ.

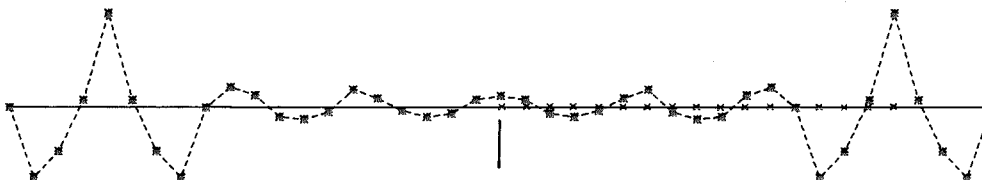
T8 = 0.690 SEC.

SAN PEDRO-TERMINAL ISLAND SUSPENSION BRIDGE  
AMBIENT VIBRATION TESTS  
SYMMETRIC VERTICAL VIBRATION



COMPUTED N. FREQUENCY = 2.340 HZ.

T9 = 0.427 SEC.

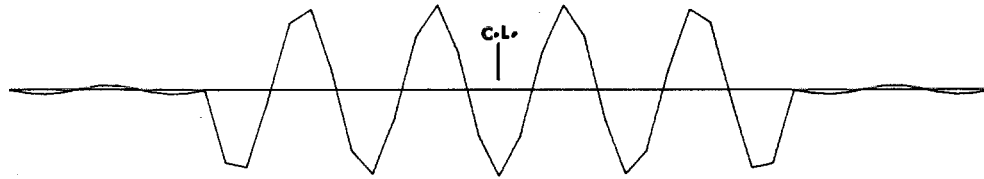


MEASURED N. FREQUENCY = 2.076 HZ.

T9 = 0.482 SEC.

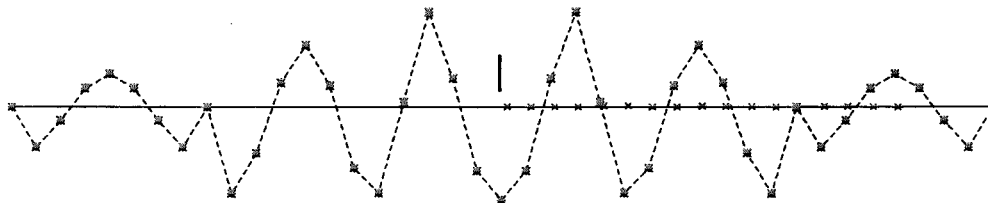
Fig. 18-d

SAN PEDRO-TERMINAL ISLAND SUSPENSION BRIDGE  
AMBIENT VIBRATION TESTS  
SYMMETRIC VERTICAL VIBRATION



COMPUTED N. FREQUENCY = 2.352 HZ.

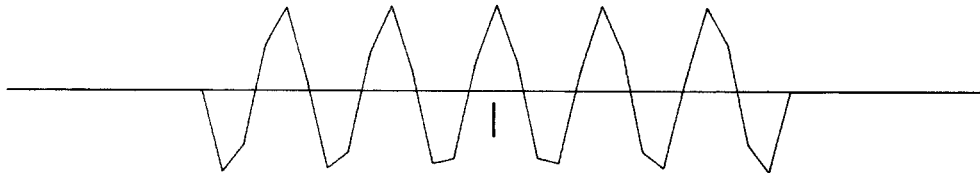
T10= 0.425 SEC.



MEASURED N. FREQUENCY = 2.146 HZ.

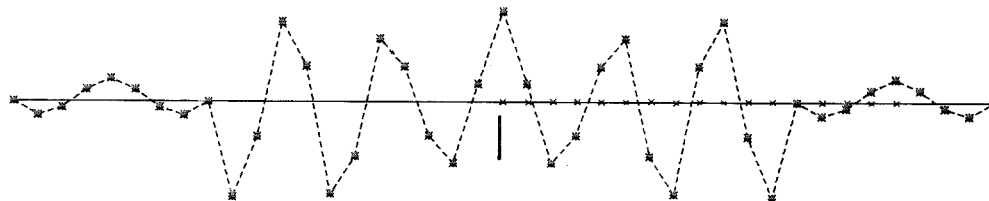
T10= 0.466 SEC.

SAN PEDRO-TERMINAL ISLAND SUSPENSION BRIDGE  
AMBIENT VIBRATION TESTS  
SYMMETRIC VERTICAL VIBRATION



COMPUTED N. FREQUENCY = 3.458 HZ.

T12= 0.289 SEC.



MEASURED N. FREQUENCY = 2.871 HZ.

T12= 0.348 SEC.

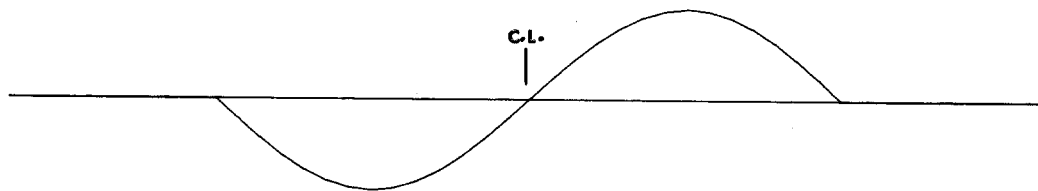
Fig. 18-e

Table 3

Comparison Between Computed and Measured Frequencies and Modes of  
Vibration of the Vincent-Thomas Suspension Bridge  
(Symmetric Vertical Vibration)

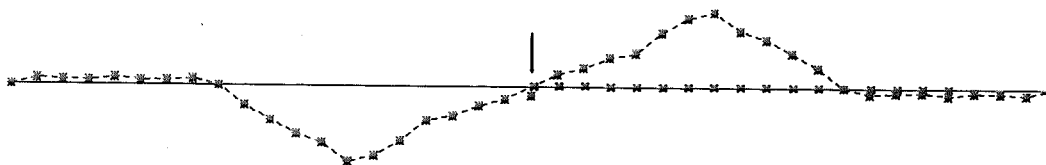
Mode	Computations		Measurements	
	Natural Freq. (Hz)	Member of Dominant Vibration	Natural Freq. (Hz)	Member of Dominant Vibration
V-S-1	0.221	Center & side spans	0.234	Center & side spans
V-S-2	0.348	Center (small motion) & side spans	0.385	Center & side spans
V-S-3	0.348	Center & side spans	0.366	Center & side spans
V-S-4	0.459	Center & side spans	0.487	Center & side spans
V-S-5	0.803	Center & side (small motion) spans	0.835	Center & side (small motion) spans
V-S-6	0.989	Towers	-	No measurements were taken
V-S-7	1.100	Side spans	1.077	Center (small motion) & side spans
V-S-8	1.467	Center span	1.450	Center span
V-S-9	2.340	Center (small motion) & side spans	2.076	Center (small motion) & side spans
V-S-10	2.352	Center & side (small motion) spans	2.146	Center & side (small motion) spans
V-S-11	3.142	Towers	-	No measurements were taken
V-S-12	3.458	Center span	2.871	Center & side (small motion) spans

SAN PEDRO-TERMINAL ISLAND SUSPENSION BRIDGE  
AMBIENT VIBRATION TESTS  
ANTISYMMETRIC VERTICAL VIBRATION



COMPUTED N. FREQUENCY = 0.197 HZ.

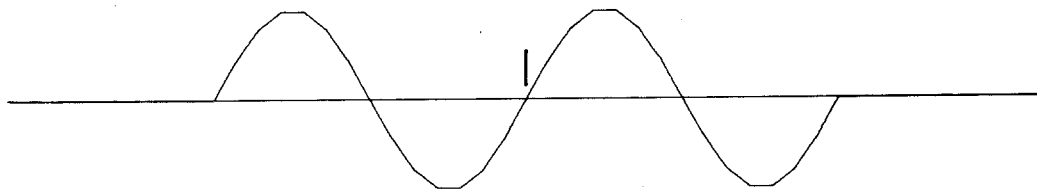
T1 = 5.076 SEC.



MEASURED N. FREQUENCY = 0.216 HZ.

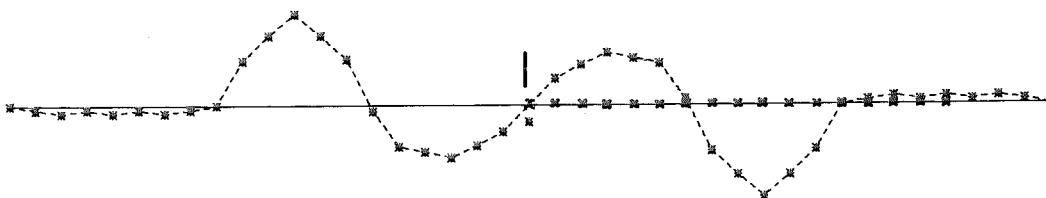
T1 = 4.630 SEC.

SAN PEDRO-TERMINAL ISLAND SUSPENSION BRIDGE  
AMBIENT VIBRATION TESTS  
ANTISYMMETRIC VERTICAL VIBRATION



COMPUTED N. FREQUENCY = 0.549 HZ.

T3 = 1.823 SEC.



MEASURED N. FREQUENCY = 0.579 HZ.

T3 = 1.727 SEC.

Fig. 19-a. Comparison between computed and measured natural frequencies and mode shapes of antisymmetric vertical vibration of the Vincent-Thomas Bridge.



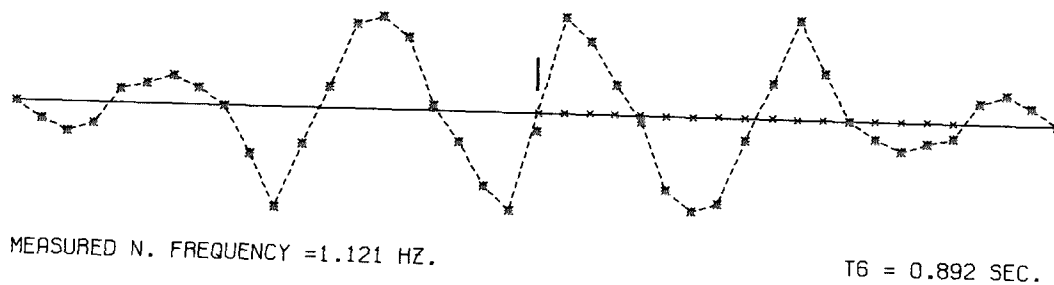
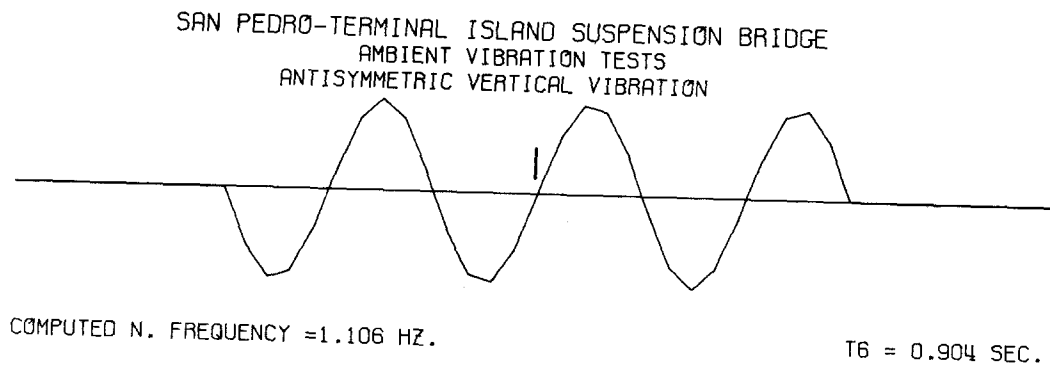
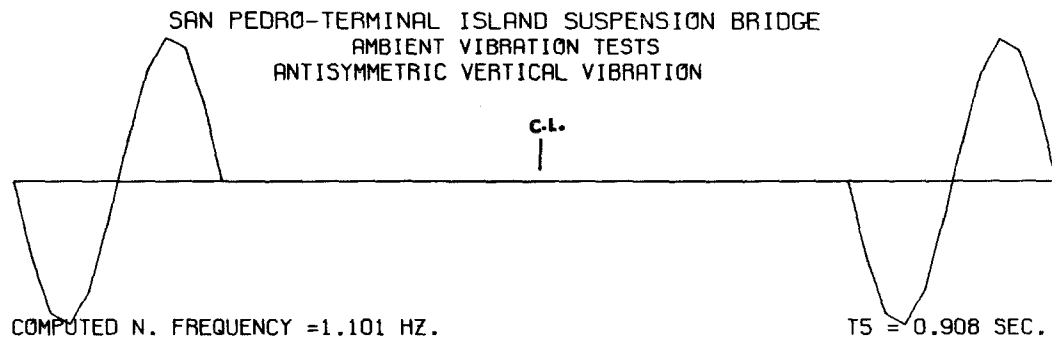
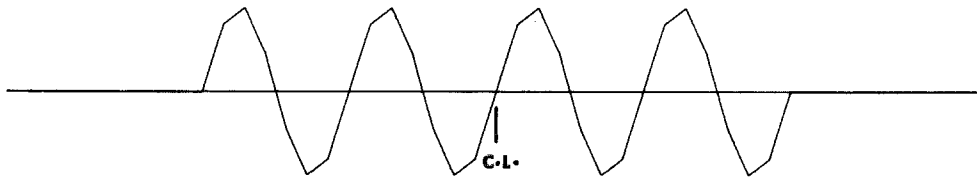


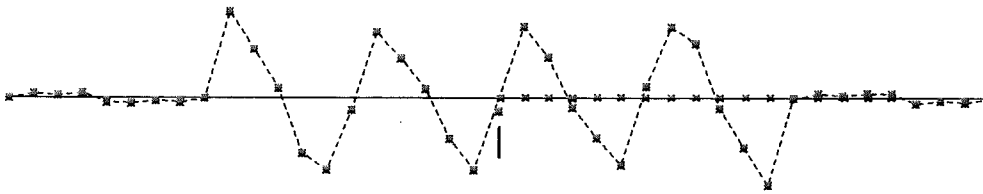
Fig. 19-b

SAN PEDRO-TERMINAL ISLAND SUSPENSION BRIDGE  
AMBIENT VIBRATION TESTS  
ANTISYMMETRIC VERTICAL VIBRATION



COMPUTED N. FREQUENCY = 1.881 HZ.

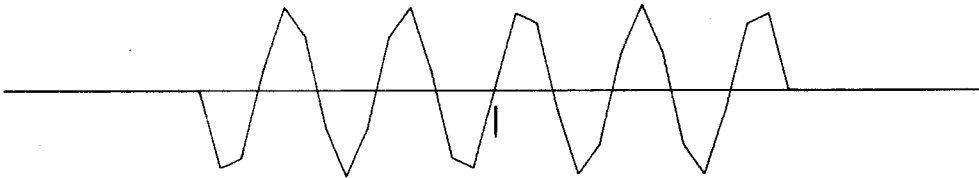
T7 = 0.532 SEC.



MEASURED N. FREQUENCY = 1.791 HZ.

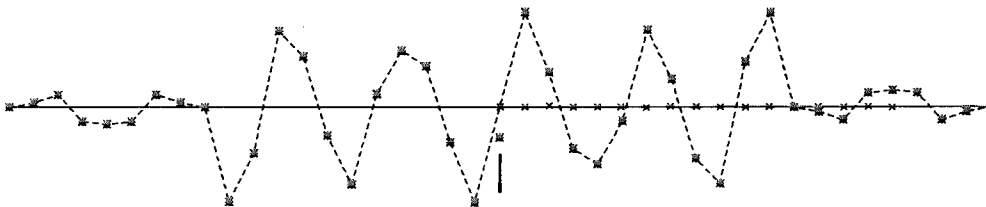
T7 = 0.558 SEC.

SAN PEDRO-TERMINAL ISLAND SUSPENSION BRIDGE  
AMBIENT VIBRATION TESTS  
ANTISYMMETRIC VERTICAL VIBRATION



COMPUTED N. FREQUENCY = 2.877 HZ.

T9 = 0.348 SEC.



MEASURED N. FREQUENCY = 2.505 HZ.

T9 = 0.399 SEC.

Fig. 19-c

Table 4

Comparison Between Computed and Measured Frequencies and Modes of  
Vibration of the Vincent-Thomas Suspension Bridge  
(Antisymmetric Vertical Vibration)

Mode	Computations		Measurements	
	Natural Frequency (Hz)	Member of Dominant Vibration	Natural Frequency (Hz)	Member of Dominant Vibration
V-AS-1	0.197	Center span	0.216	Center span
V-AS-2	0.346	Side spans	-	It could be the measured mode V-S-2
V-AS-3	0.549	Center span	0.579	Center span
V-AS-4	0.989	Towers	-	No measurements were taken
V-AS-5	1.101	Side spans	1.022	Center (small motion) & side spans
V-AS-6	1.106	Center span	1.121	Center & side (small motion) spans
V-AS-7	1.881	Center span	1.791	Center span
V-AS-8	2.338	Side spans	-	It could be the measured mode V-S-9
V-AS-9	2.877	Center span	2.505	Center & side (small motion) spans

## 2. Torsional Vibration

The agreement between computed and measured mode shapes and natural frequencies for both symmetric and antisymmetric vibrations is surprisingly good for torsional vibration. In the literature, most of the dynamic tests on suspension bridges indicate that torsional modes are more difficult to identify experimentally (Refs. 1 and 2) and may require more favorable conditions for their measurements. Also, in past tests large differences were encountered between the computed and measured torsional modes. This may be due to the difficulty in achieving realistic estimates for the torsional stiffness of the stiffening structure and perhaps also to the observed coupled vertical-torsional motion during the structural testing.

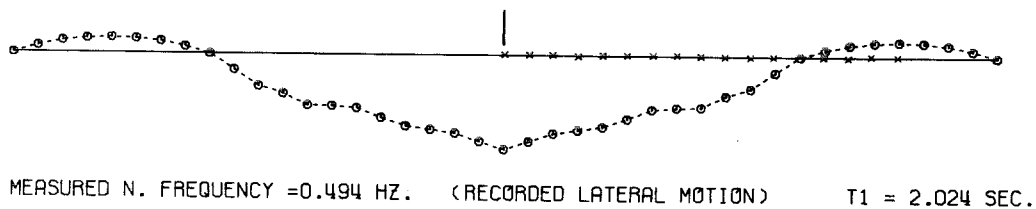
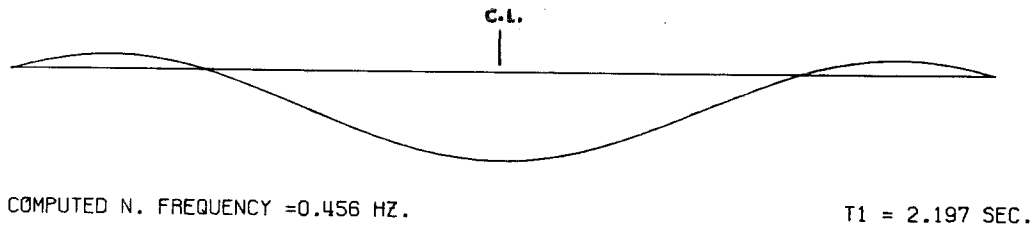
As mentioned previously, all the torsional modes were recovered from the recorded lateral motion, whereas only 4 out of 6 symmetric modes and 2 out of 5 antisymmetric modes were recovered from the recorded vertical motions (Figs. 20 and 21). The lateral and torsional vibrational modes are well separated in the frequency domain, although some torsional modes were very close to some vertical modes, and their separation was troublesome. As in the vertical vibration, there is still some interaction or coupled motion between the side and the center spans in the higher modes.

As discussed before in the vertical vibration case, the computed sixth symmetric mode, T-S-6, (2.407 Hz) and the computed fourth antisymmetric mode, T-AS-4, (2.407 Hz) are identical

except for the fact that in the symmetric case the two side spans are moving in-phase while in the antisymmetric case they are moving  $180^\circ$  out-of-phase. This suggests that the measured fourth antisymmetric mode could be representative of the sixth symmetric mode shape.

Tables 5 and 6 show the comparison between the computed and measured frequencies and modes of torsional vibration.

SAN PEDRO-TERMINAL ISLAND SUSPENSION BRIDGE  
 AMBIENT VIBRATION TESTS  
 SYMMETRIC TORSIONAL VIBRATION



SAN PEDRO-TERMINAL ISLAND SUSPENSION BRIDGE  
 AMBIENT VIBRATION TESTS  
 SYMMETRIC TORSIONAL VIBRATION

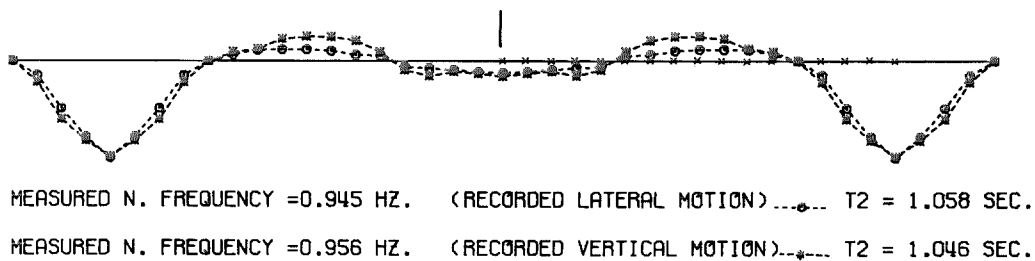
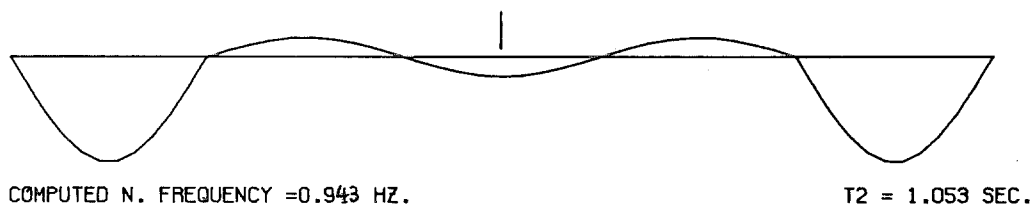
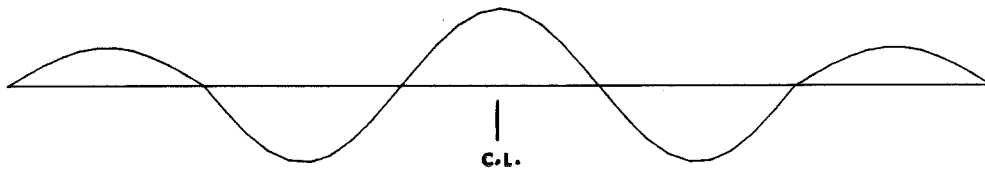


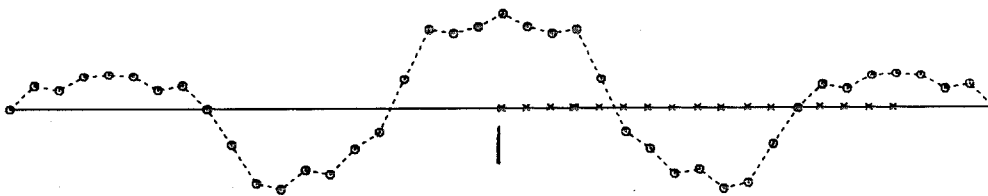
Fig. 20-a. Comparison between computed and measured natural frequencies and mode shapes of symmetric torsional vibration of the Vincent-Thomas Bridge.

SAN PEDRO-TERMINAL ISLAND SUSPENSION BRIDGE  
 AMBIENT VIBRATION TESTS  
 SYMMETRIC TORSIONAL VIBRATION



COMPUTED N. FREQUENCY = 0.950 HZ.

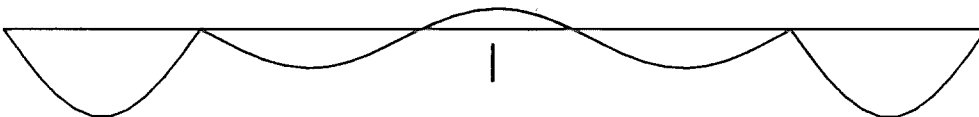
T3 = 1.052 SEC.



MEASURED N. FREQUENCY = 1.069 HZ. (RECORDED LATERAL MOTION)

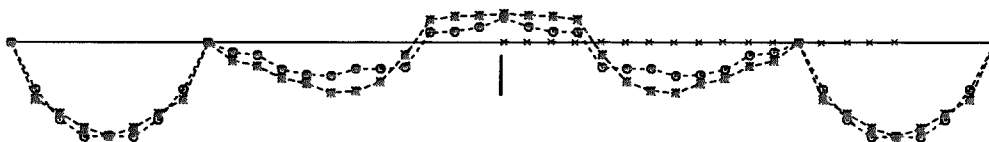
T3 = 0.935 SEC.

SAN PEDRO-TERMINAL ISLAND SUSPENSION BRIDGE  
 AMBIENT VIBRATION TESTS  
 SYMMETRIC TORSIONAL VIBRATION



COMPUTED N. FREQUENCY = 1.012 HZ.

T4 = 0.988 SEC.

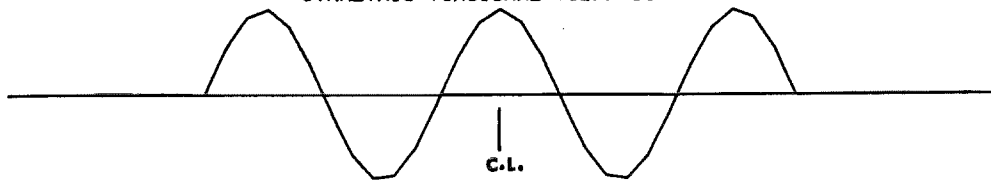


MEASURED N. FREQUENCY = 1.018 HZ. (RECORDED LATERAL MOTION)..... T4 = 0.982 SEC.

MEASURED N. FREQUENCY = 1.018 HZ. (RECORDED VERTICAL MOTION)..... T4 = 0.982 SEC.

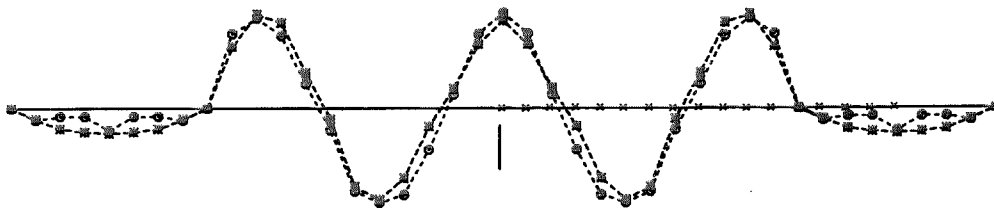
Fig. 20-b

SAN PEDRO-TERMINAL ISLAND SUSPENSION BRIDGE  
AMBIENT VIBRATION TESTS  
SYMMETRIC TORSIONAL VIBRATION



COMPUTED N. FREQUENCY = 1.857 HZ.

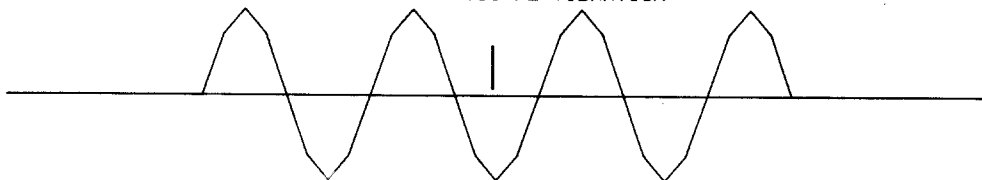
T5 = 0.539 SEC.



MEASURED N. FREQUENCY = 1.893 HZ. (RECORDED LATERAL MOTION) ---○--- T5 = 0.528 SEC.

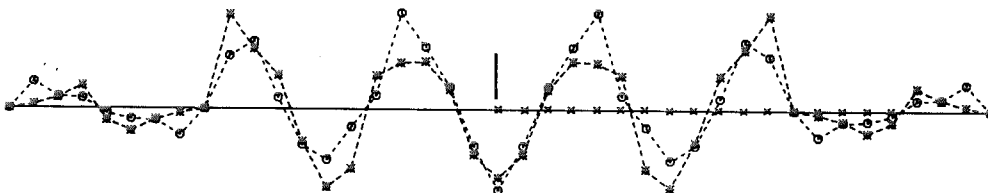
MEASURED N. FREQUENCY = 1.893 HZ. (RECORDED VERTICAL MOTION) ---×--- T5 = 0.528 SEC.

SAN PEDRO-TERMINAL ISLAND SUSPENSION BRIDGE  
AMBIENT VIBRATION TESTS  
SYMMETRIC TORSIONAL VIBRATION



COMPUTED N. FREQUENCY = 3.079 HZ.

T7 = 0.325 SEC.



MEASURED N. FREQUENCY = 2.791 HZ. (RECORDED LATERAL MOTION) ---○--- T7 = 0.358 SEC.

MEASURED N. FREQUENCY = 2.780 HZ. (RECORDED VERTICAL MOTION) ---×--- T7 = 0.360 SEC.

Fig. 20-c

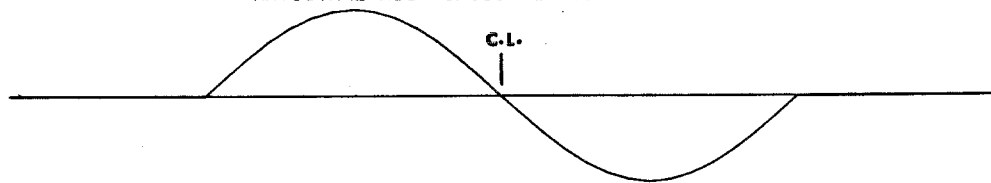


Table 5

Comparison Between Computed and Measured Frequencies and Modes of  
Vibration of the Vincent-Thomas Suspension Bridge  
(Symmetric Torsional Vibration)

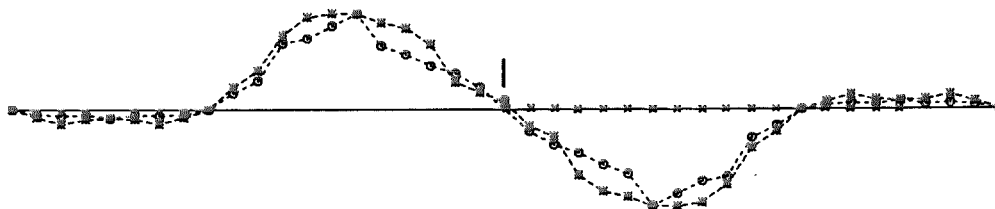
Mode	Computations		Measurements		
	Natural Frequency (Hz)	Member of Dominant Vibration	Natural Frequency (Hz)		Member of Dominant Vibration
			Lateral Motion	Vertical Motion	
T-S-1	0.456	Center & side spans	0.494	-	Center & side spans
T-S-2	0.943	Center & side spans	0.945	0.956	Center & side spans
T-S-3	0.950	Center & side spans	1.069	-	Center & side spans
T-S-4	1.012	Center & side spans	1.018	1.018	Center & side spans
T-S-5	1.857	Center span	1.893	1.893	Center & side (small motion) spans
T-S-6	2.407	Side spans	-	-	It could be the measured mode T-AS-4
T-S-7	3.079	Center span	2.791	2.780	Center & side (small motion) spans

SAN PEDRO-TERMINAL ISLAND SUSPENSION BRIDGE  
 AMBIENT VIBRATION TESTS  
 ANTISYMMETRIC TORSIONAL VIBRATION



COMPUTED N. FREQUENCY = 0.596 HZ.

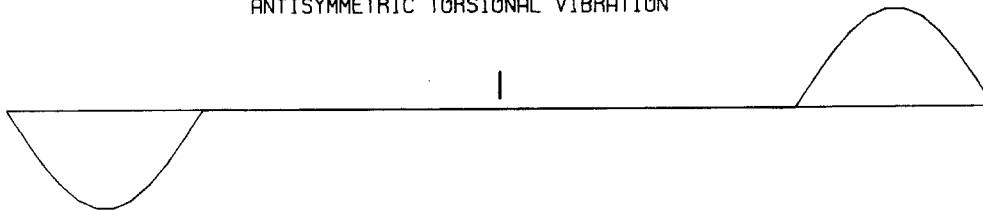
T1 = 1.678 SEC.



MEASURED N. FREQUENCY = 0.740 HZ. (RECORDED LATERAL MOTION) T1 = 1.351 SEC.

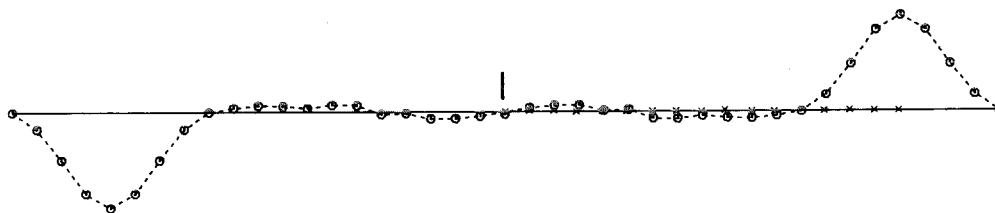
MEASURED N. FREQUENCY = 0.740 HZ. (RECORDED VERTICAL MOTION) T1 = 1.351 SEC.

SAN PEDRO-TERMINAL ISLAND SUSPENSION BRIDGE  
 AMBIENT VIBRATION TESTS  
 ANTISYMMETRIC TORSIONAL VIBRATION



COMPUTED N. FREQUENCY = 0.944 HZ.

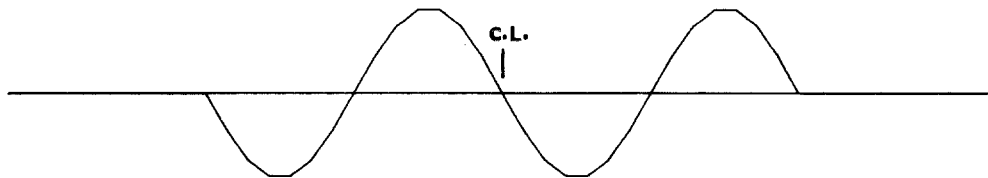
T2 = 1.059 SEC.



MEASURED N. FREQUENCY = 0.806 HZ. (RECORDED LATERAL MOTION) T2 = 1.241 SEC.

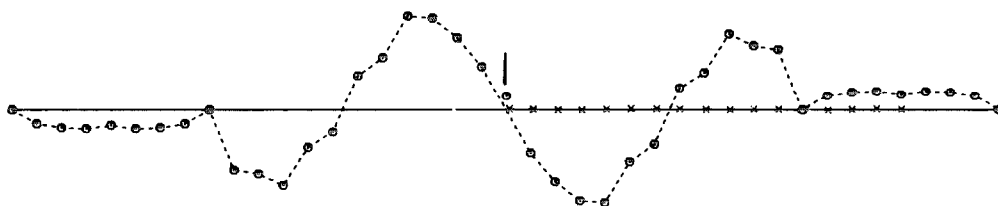
Fig. 21-a. Comparison between computed and measured natural frequencies and mode shapes of antisymmetric torsional vibration of the Vincent-Thomas Bridge.

SAN PEDRO-TERMINAL ISLAND SUSPENSION BRIDGE  
 AMBIENT VIBRATION TESTS  
 ANTISYMMETRIC TORSIONAL VIBRATION



COMPUTED N. FREQUENCY = 1.367 HZ.

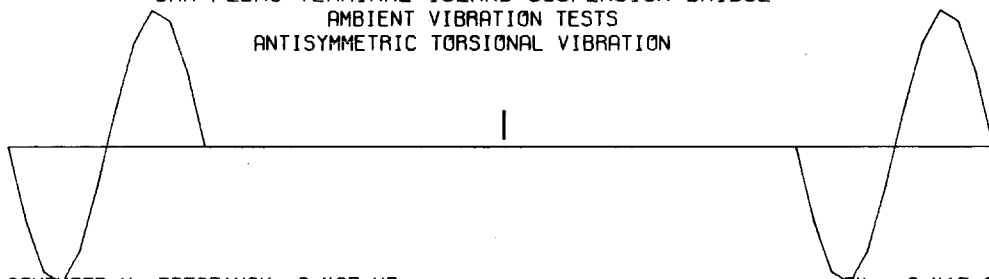
T3 = 0.732 SEC.



MEASURED N. FREQUENCY = 1.425 HZ. (RECORDED LATERAL MOTION)

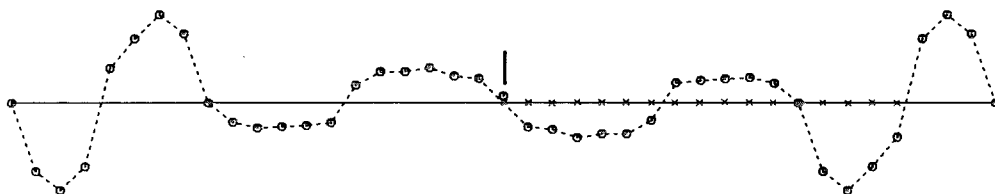
T3 = 0.702 SEC.

SAN PEDRO-TERMINAL ISLAND SUSPENSION BRIDGE  
 AMBIENT VIBRATION TESTS  
 ANTISYMMETRIC TORSIONAL VIBRATION



COMPUTED N. FREQUENCY = 2.407 HZ.

T4 = 0.415 SEC.

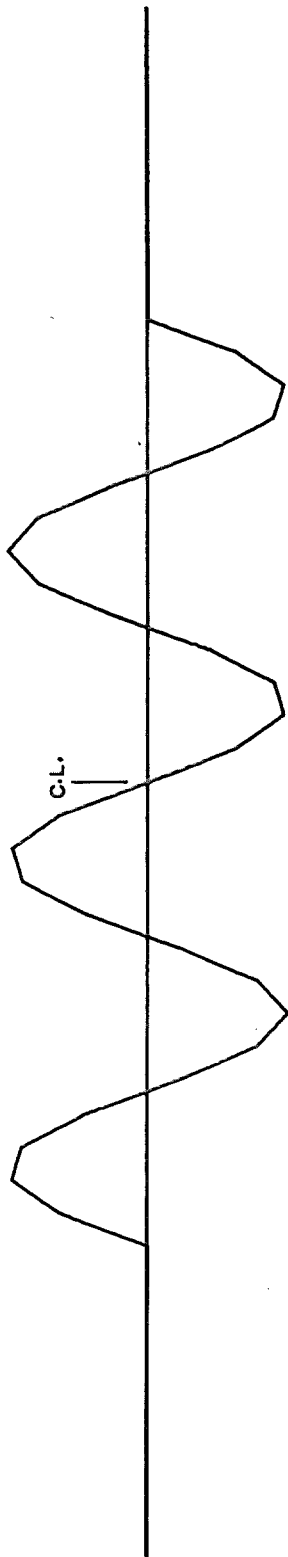


MEASURED N. FREQUENCY = 2.109 HZ. (RECORDED LATERAL MOTION)

T4 = 0.474 SEC.

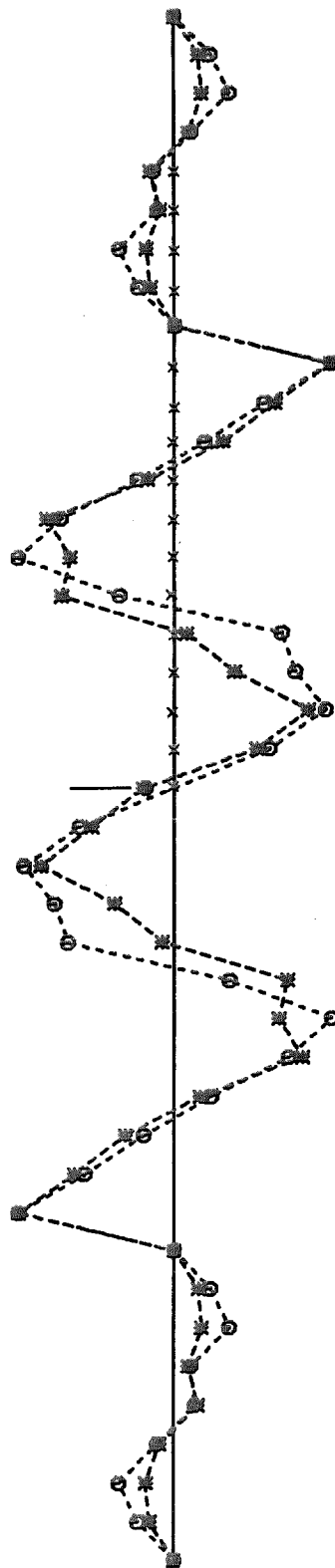
Fig. 21-b

SAN PEDRO-TERMINAL ISLAND SUSPENSION BRIDGE  
 AMBIENT VIBRATION TESTS  
 ANTISYMMETRIC TORSIONAL VIBRATION



COMPUTED N. FREQUENCY = 2.424 HZ.

$T_5 = 0.413 \text{ SEC.}$



MEASURED N. FREQUENCY = 2.344 HZ. (RECORDED LATERAL MOTION)  $T_5 = 0.427 \text{ SEC.}$

MEASURED N. FREQUENCY = 2.344 HZ. (RECORDED VERTICAL MOTION)  $T_5 = 0.427 \text{ SEC.}$

Table 6

Comparison Between Computed and Measured Frequencies and Modes of  
Vibration of the Vincent-Thomas Suspension Bridge  
(Antisymmetric Torsional Vibration)

Mode	Computations		Measurements		
	Natural Frequency (Hz)	Member of Dominant Vibration	Natural Frequency (Hz)		Member of Dominant Vibration
			Lateral Motion	Vertical Motion	
T-AS-1	0.596	Center span	0.740	0.740	Center & side (small motion) spans
T-AS-2	0.944	Side spans	0.806	-	Center (small motion) & side spans
T-AS-3	1.367	Center span	1.425	-	Center & side (small motion) spans
T-AS-4	2.407	Side spans	2.109	-	Center (small motion) & side spans
T-AS-5	2.424	Center span	2.344	2.344	Center & side (small motion) spans

### 3. Lateral Vibration

The lateral motion of the cable itself was not recorded, so a detailed comparison between measured and computed lateral mode shapes and frequencies was not possible. However, the recorded lateral motion of the stiffening structure enables the making of meaningful comparisons between the computations and the measurements of lateral vibration.

The mode shapes and frequencies of lateral vibration were computed for only the center span of the Vincent-Thomas suspension bridge by the finite-element method.<sup>3</sup> However, for the sake of a complete comparison the first and the second lateral modes of the side spans were computed by an approximate method developed in Ref. 3.

Figures 22, 23 and 24 indicate reasonable agreement for both the center span and the side spans; however, these figures also point out the interaction phenomena between the side and the center spans. This interaction has been neglected in the analysis for lateral vibration in order to stay within the linear theory of small vibrational amplitudes.

The computation of the lateral modes of vibration of the Vincent-Thomas Bridge shows that the first two symmetric lateral modes have similar configurations except for the fact that in the first mode the cable and the suspended structure are moving in phase, while in the second mode they are moving  $180^\circ$  out-of-phase (see Fig. 22-a). The same situation was discovered in the case of

the first two computed antisymmetric lateral modes. The measurements identified the first two symmetric lateral modes (Fig. 22-a), and only the in-phase antisymmetric lateral mode. There is a possibility that the  $180^\circ$  out-of-phase antisymmetric lateral mode was coupled with the first measured lateral mode of the side span as shown in Fig. 24, where relatively large vibrational amplitudes of the center span have been measured. It is important to note that the modal amplitudes shown in Fig. 24 are absolute, i. e., either symmetric or antisymmetric motion is possible, since measurements were taken only on half of the bridge.

Table 7 contains the comparison between the computations and the measurements of the lateral symmetric and antisymmetric modes of vibration.

Finally, it should also be noted that in lateral vibration there are upward vibrational displacements of the cables and the suspended structure incidental to their lateral movements; that is, the cable and suspended structure move with a pendular action. Evidence of these upward deflections has been found in the Fourier spectra of the recorded vertical motion as indicated by the arrows in Figs. 13 and 15 and also in Figs. A-1 and A-3 in Appendix A. The peaks of these upward motions are at 0.54 Hz, 0.88 Hz, 1.20 Hz, 1.53 Hz and 2.64 Hz which correspond to the lateral modes L-S-2, L-S-3, L-S-4, L-S-5 and L-AS-6, respectively.

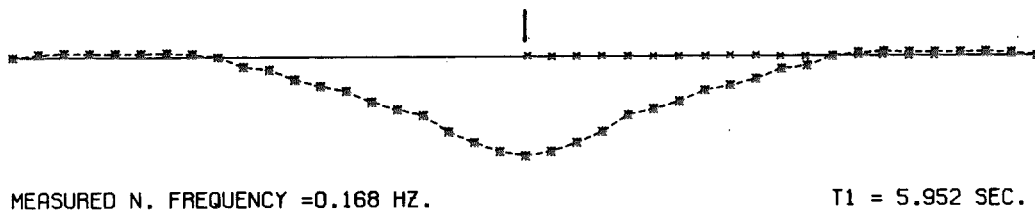
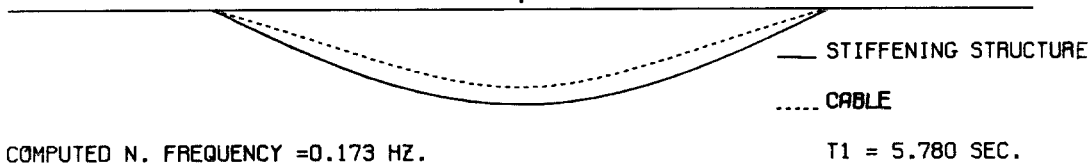
In general, Fig. 25, which summarizes the comparison between the computed and measured frequencies and modes for vertical,

torsional and lateral vibrations, shows quite good agreement which confirms the validity of the method of dynamic analysis developed for suspension bridges and also confirms the reliability of the measurements.



SAN PEDRO-TERMINAL ISLAND SUSPENSION BRIDGE  
AMBIENT VIBRATION TESTS  
SYMMETRIC LATERAL VIBRATION

C.L.



SAN PEDRO-TERMINAL ISLAND SUSPENSION BRIDGE  
AMBIENT VIBRATION TESTS  
SYMMETRIC LATERAL VIBRATION

C.L.

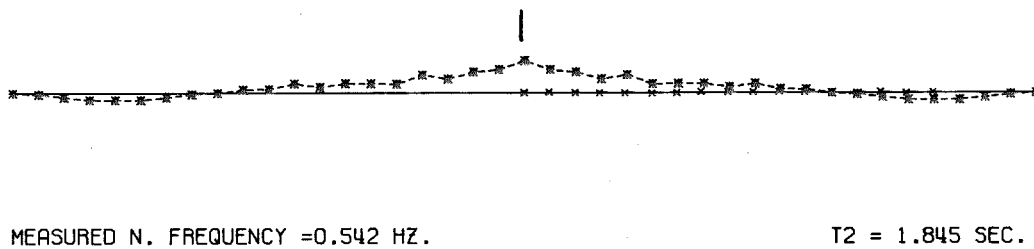
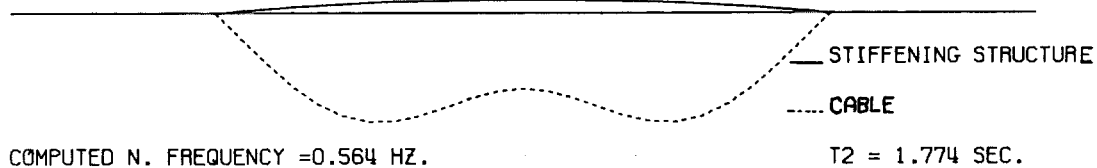
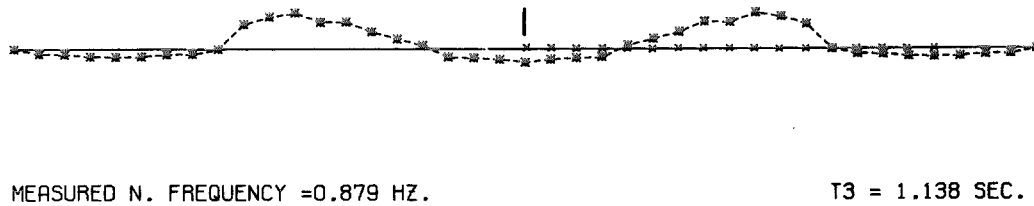
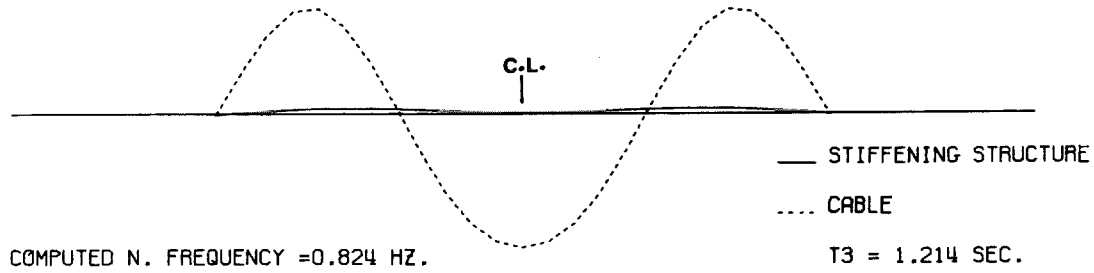


Fig. 22-a. Comparison between computed and measured natural frequencies and mode shapes of symmetric lateral vibration of the stiffening structure (center span) of the Vincent-Thomas Bridge.

SAN PEDRO-TERMINAL ISLAND SUSPENSION BRIDGE  
AMBIENT VIBRATION TESTS



SAN PEDRO-TERMINAL ISLAND SUSPENSION BRIDGE  
AMBIENT VIBRATION TESTS  
SYMMETRIC LATERAL VIBRATION

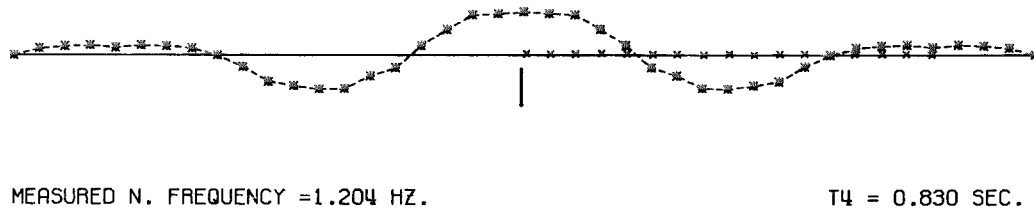
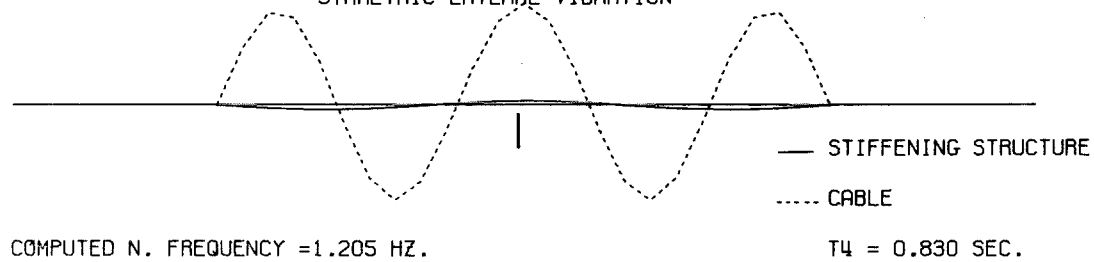
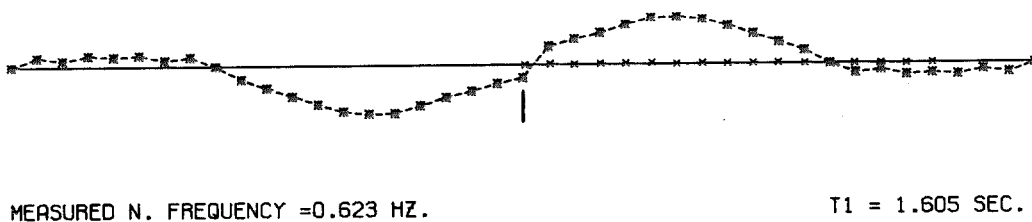
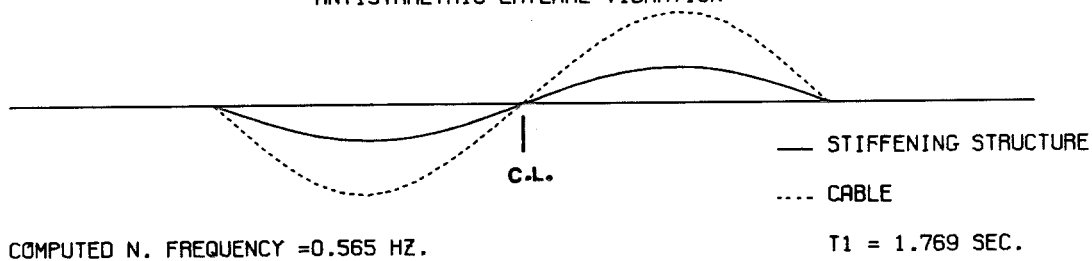


Fig. 22-b

SAN PEDRO-TERMINAL ISLAND SUSPENSION BRIDGE  
 AMBIENT VIBRATION TESTS  
 ANTISYMMETRIC LATERAL VIBRATION



SAN PEDRO-TERMINAL ISLAND SUSPENSION BRIDGE  
 AMBIENT VIBRATION TESTS  
 ANTISYMMETRIC LATERAL VIBRATION

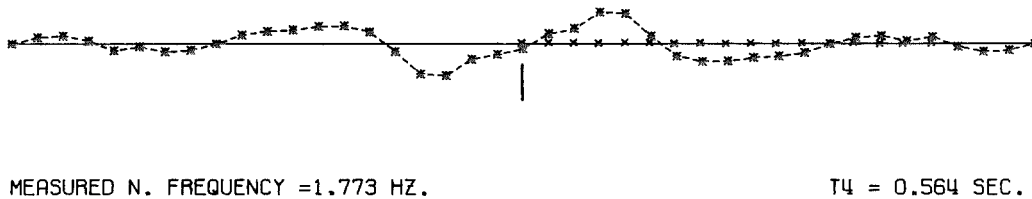
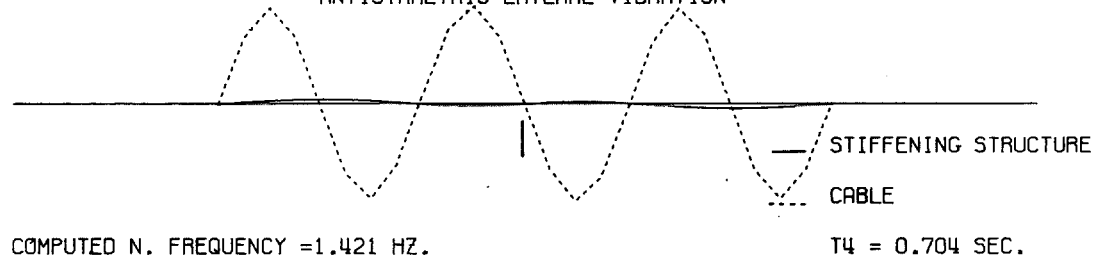
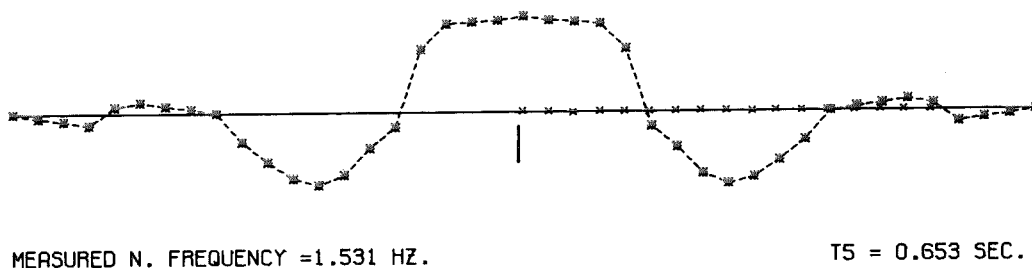
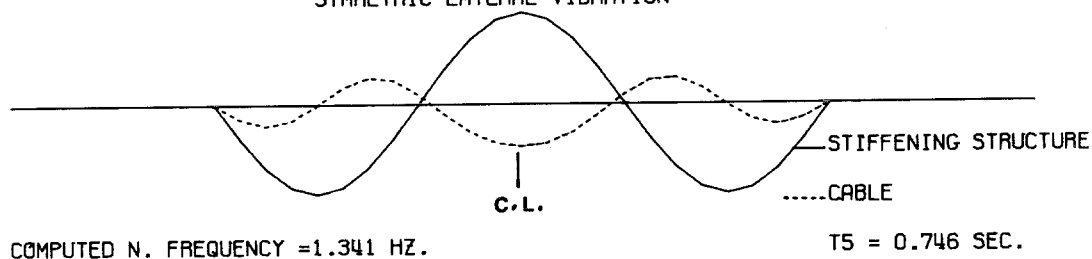


Fig. 23-a. Comparison between computed and measured natural frequencies and mode shapes of antisymmetric lateral vibration of the stiffening structure (center span) of the Vincent-Thomas Bridge.

SAN PEDRO-TERMINAL ISLAND SUSPENSION BRIDGE  
 AMBIENT VIBRATION TESTS  
 SYMMETRIC LATERAL VIBRATION



SAN PEDRO-TERMINAL ISLAND SUSPENSION BRIDGE  
 AMBIENT VIBRATION TESTS  
 ANTISYMMETRIC LATERAL VIBRATION

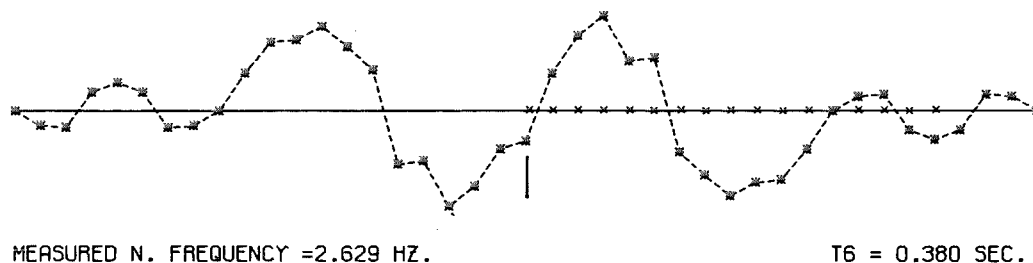
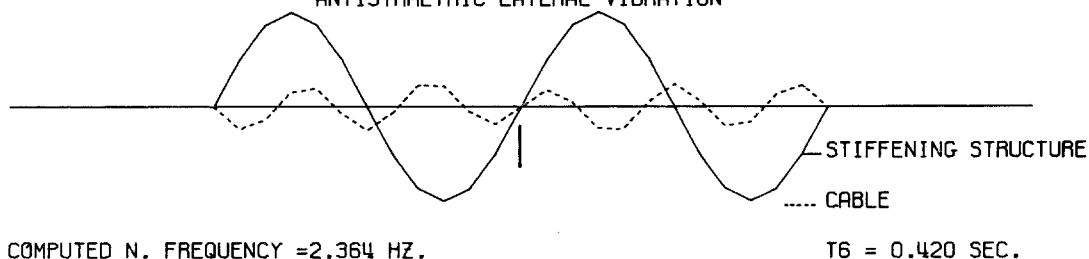
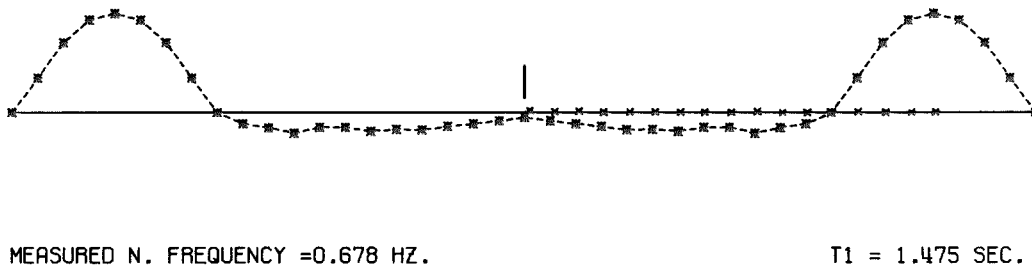
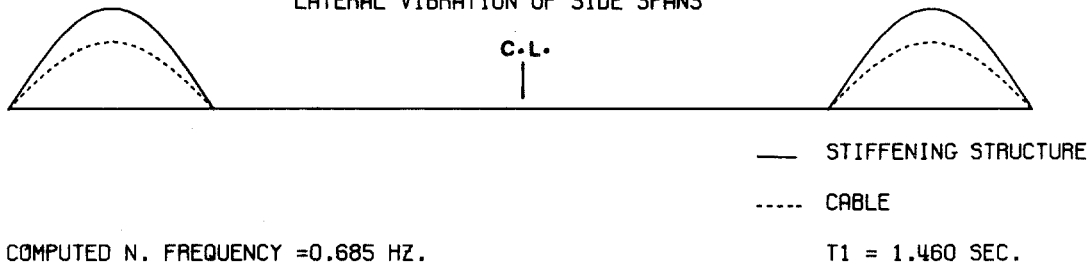


Fig. 23-b. Comparison between computed and measured natural frequencies and mode shapes of lateral vibration of the stiffening structure (center span) of the Vincent-Thomas Bridge.

SAN PEDRO-TERMINAL ISLAND SUSPENSION BRIDGE  
 AMBIENT VIBRATION TESTS  
 LATERAL VIBRATION OF SIDE SPANS



SAN PEDRO-TERMINAL ISLAND SUSPENSION BRIDGE  
 AMBIENT VIBRATION TESTS  
 LATERAL VIBRATION OF SIDE SPANS

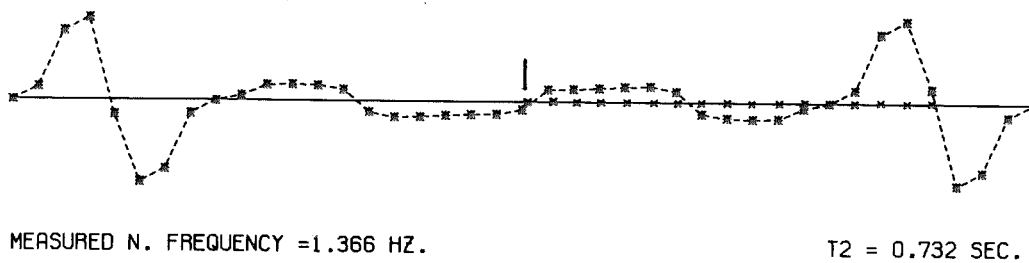
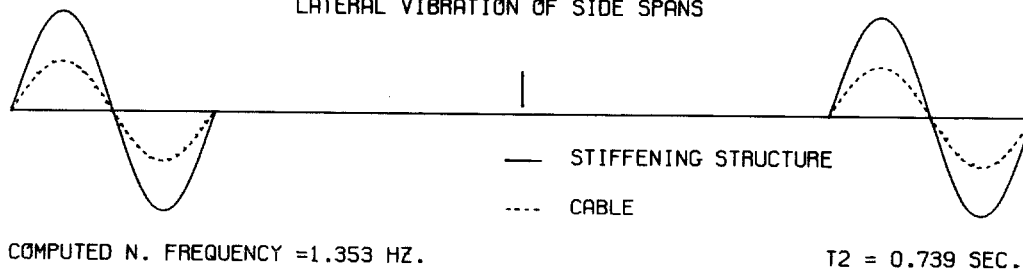


Fig. 24. Comparison between computed and measured natural frequencies and mode shapes of lateral vibration of the stiffening structure (side spans) of the Vincent-Thomas Bridge.

Table 7

Comparison Between Computed and Measured Frequencies and Modes of  
Vibration of the Vincent-Thomas Suspension Bridge  
(Lateral Vibration)

Types of Vibration	Mode	Computations		Measurements	
		Natural Frequency (Hz)	Member of Dominant Vibration	Natural Frequency (Hz)	Member of Dominant Vibration
Symmetric (Center Span)	L-S-1	0.173	Suspended structure & cable	0.168	Suspended structure
	L-S-2	0.564	Suspended structure & cable	0.542	Suspended structure
	L-S-3	0.824	Suspended structure (small motion) & cable	0.879	Suspended structure & side spans (small motion)
	L-S-4	1.205	Suspended structure (small motion) & cable	1.204	Suspended structure & side spans (small motion)
	L-S-5	1.341	Suspended structure & cable	1.531	Suspended structure & side spans (small motion)
Antisymmetric (Center Span)	L-AS-1	0.565	Suspended structure & cable	0.623	Suspended structure & side spans (small motion)
	L-AS-2	0.643	Suspended structure & cable	-	No measurements were taken
	L-AS-3	0.996	Cable	-	
	L-AS-4	1.421	Suspended structure (small motion) & cable	1.773	Suspended structure & side spans (small motion)
	L-AS-5	1.882	Cable	-	No measurements were taken
	L-AS-6	2.364	Suspended structure & cable	2.629	
Side Spans	1	0.685	Suspended structure & cable	0.678	Suspended structure & center span (small motion)
	2	1.353	Suspended structure & cable	1.366	Suspended structure & center span (small motion)

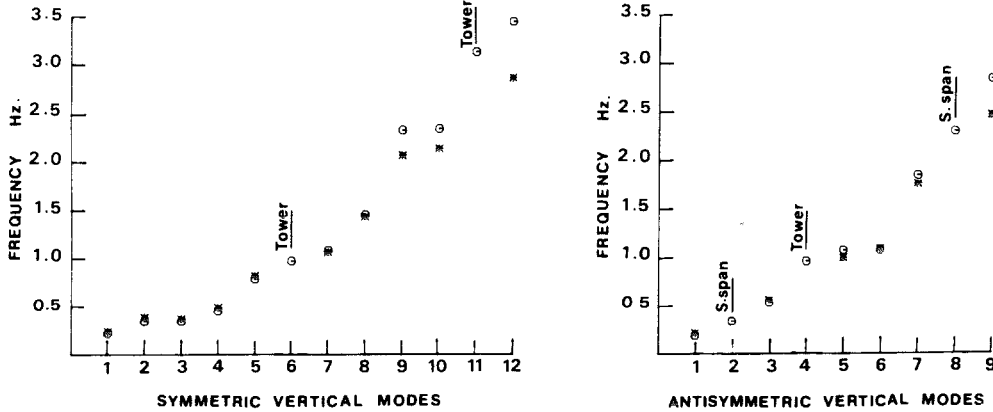
Notes:

1. Measurements were taken only on the suspended structure for both center span and side spans of the bridge.

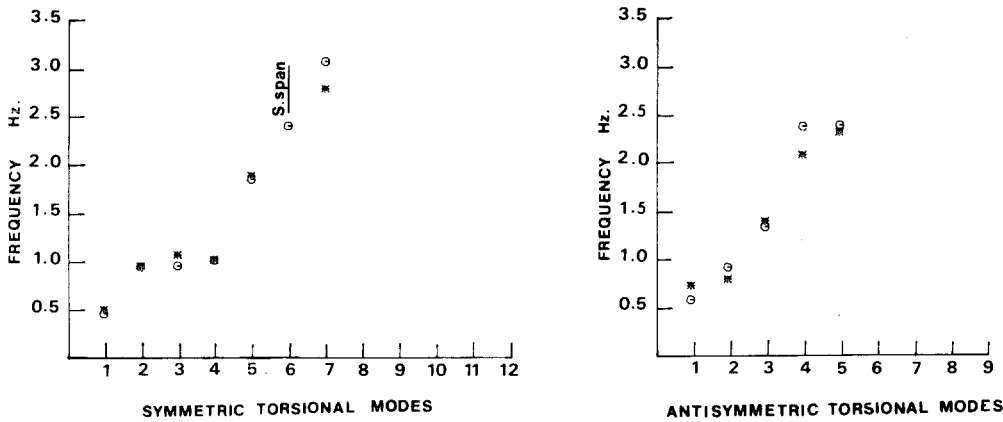
# SAN PEDRO-TERMINAL ISLAND SUSPENSION BRIDGE

## AMBIENT VIBRATION TESTS

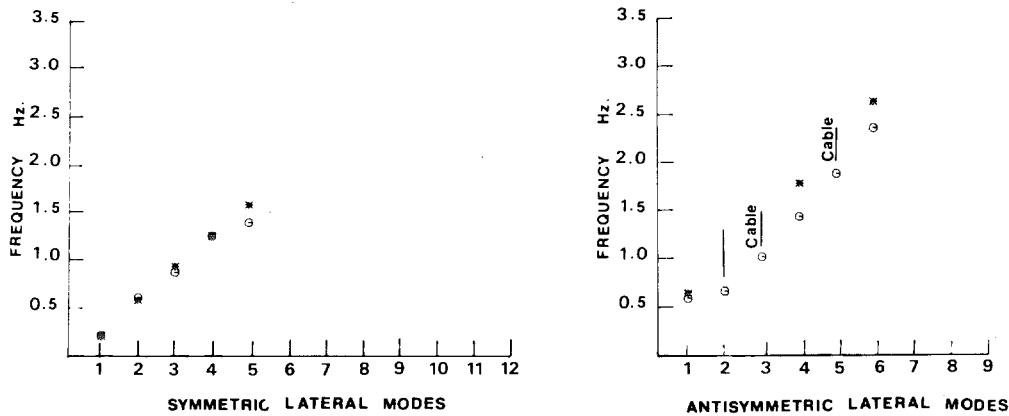
### VERTICAL VIBRATION



### TORSIONAL VIBRATION



### LATERAL VIBRATION



○ COMPUTED FREQUENCIES

\* MEASURED FREQUENCIES

Fig. 25. Comparison between computed and measured frequencies for vertical, torsional and lateral modes of vibration.

### DAMPING

Although forced vibration tests would possibly yield the most reliable values of damping belonging to each mode of vibration, standard tests are impractical for this type of structure. However, the vibration decay from simulated impacts applied to a suspension bridge with no traffic can be used to obtain damping values, as did Rainer and Selst<sup>2</sup> in their tests.

Estimated damping values from ambient vibration tests could be obtained by the method of half-power bandwidth of the Fourier spectrum peaks. But, it is unlikely that an accurate estimate will be obtained. Several factors contribute to errors in the computed damping values. Firstly, the vibration of the bridge when vehicles are passing over it is a non-stationary random process which can broaden the bandwidth of the response peak and thus yield damping values that may be too high. Secondly, the presence of adjacent peaks in the spectrum either due to closely spaced modal peaks or due to spectral overlap can cause difficulty in estimating damping values. Thirdly, for some of the modes it is difficult to find a spectral peak whose width can be properly measured. Finally, the smoothing process of the Fourier spectra could contribute to the overestimation of damping by diminishing the spectral peaks and broadening the bandwidth at the half-power points. Also, averaging a number of sequential spectral peaks may be highly desirable for a proper definition of the spectral peaks, but this could lead to wider peaks due to the slight frequency shift.



Because of these factors, satisfactory estimation of damping values was not possible; however, the range of the damping-ratio values of each measured mode was calculated from the results obtained and is presented in Table 8.

Table 8  
Range of the Damping Ratios of the Measured Modes of Vibrations  
of the Vincent-Thomas Suspension Bridge

Vertical Vibration				Torsional Vibration				Lateral Vibration			
Symmetric		Antisymmetric		Symmetric		Antisymmetric		Symmetric		Antisymmetric	
Mode	Damping Ratio	Mode	Damping Ratio	Mode	Damping Ratio	Mode	Damping Ratio	Mode	Damping Ratio	Mode	Damping Ratio
1	0.0215 ~ 0.0235	1	0.0139 ~ 0.0185	1	0.0071 ~ 0.0092	1	0.0045 ~ 0.0068	1	0.0195 ~ 0.0283	1	0.0048 ~ 0.0052
2	0.0105 ~ 0.0158	3	0.0048 ~ 0.0060	2	0.0042 ~ 0.0047	2	0.0040 ~ 0.0059	2	0.0088 ~ 0.0102	4	0.0040 ~ 0.0050
3	0.0068 ~ 0.0109	5	0.0042 ~ 0.0055	3	0.0030 ~ 0.0035	3	0.0021 ~ 0.0039	3	0.0040 ~ 0.0063	6	0.0022 ~ 0.0029
4	0.0077 ~ 0.0103	6	0.0035 ~ 0.0053	4	0.0042 ~ 0.0051	4	0.0023 ~ 0.0038	4	0.0029 ~ 0.0058	2*	0.0035 ~ 0.0052
5	0.0070 ~ 0.0087	7	0.0021 ~ 0.0028	5	0.0019 ~ 0.0030	5	0.0018 ~ 0.0030	5	0.0028 ~ 0.0043		
7	0.0037 ~ 0.0050	9	0.0020 ~ 0.0024	7	0.0016 ~ 0.0025			1*	0.0072 ~ 0.0081		
8	0.0039 ~ 0.0045										
9	0.0019 ~ 0.0027										
10	0.0023 ~ 0.0032										
12	0.0021 ~ 0.0024										

\* Lateral vibration of the side spans.

\*\* Damping ratio is calculated by the half-power (bandwidth) method.

## CONCLUSIONS

This study is concerned with the measurement of the dynamic response of the Vincent-Thomas Suspension Bridge (Los Angeles Harbor) to excitations by vehicular traffic. The measurements identified sixteen vertical modes, eleven torsional modes and ten lateral modes and their natural frequencies, in the frequency range 0.0 Hz to 3.0 Hz. These frequencies and mode shapes were determined for small amplitude vibrations and, hence, indicate the structural behavior in the range of linear response. However, the measurements also demonstrated an interaction between side and center spans in the higher as well as the lower modes of vibration which indicate non-linear behavior.

Good modal identification was achieved by special deployment and orientation of the motion-sensing instruments and by summing and subtracting records to enhance vertical motions and torsional motions. Relatively long time intervals were recorded which contributed to higher resolution of the Fourier spectra. Consequently, better determination of the closely spaced modes of vibration was obtained. The characteristics of torsional modes were well-determined from recorded lateral motion. The vertical component of the torsional motion was not so well obtained and only six out of eleven torsional modes were recovered from the recorded vertical motions; the other five torsional modes were very close to vertical modes which dominated the vertical motion.

It was not possible to determine reliable damping values adequately by use of the half-power method due to closely spaced

peaks and to spectral overlap which resulted in widening of the Fourier spectrum peaks; however, a rough estimation of the damping ratios was presented.

Finally, this comparison between measured and computed natural frequencies and mode shapes suggests for future earthquake-resistance analyses that computed values can, indeed, be representative of the real structure.

It is recommended that four strong motion accelerographs be installed at the Vincent Thomas Bridge to record future earthquake motions. One should be installed at the base of one of the towers; one should be installed at the intersection of the deck and the tower; and the third and fourth should be installed at the third point of both the center span and side span.

### ACKNOWLEDGEMENT

The authors wish to thank the Vincent-Thomas Suspension Bridge Authority team, under the supervision of Mr. Daniel C. Butler, for the time and effort they contributed to the taking of the field measurements on the 23rd and 24th of September 1976. The assistance provided by Mr. Raul Relles in operating and maintaining the instrumentation system, in conducting the tests and also in reducing the data is greatly appreciated. Gratitude is also extended to Mr. A. Brooks, Mr. M. Haroun, Mr. B. Herring, Mr. Sai-Man Li and Mr. W. Yeung, members of Caltech team who provided great assistance in conducting the tests.

We are indebted also to Professor P. C. Jennings of the California Institute of Technology for critical reading of the text and for his valuable suggestions.

This research was supported by grants from the National Science Foundation and the Earthquake Research Affiliates Program at the California Institute of Technology.

## REFERENCES

1. McLamore, V.R., Hart, G.C. and Stubbs, I.R., "Ambient Vibration of Two Suspension Bridges", Journal of Structural Division, Proc. Am. Soc. of C.E., ST10, October 1971, pp. 2567-2582.
2. Rainer, J.H. and Selst, V.A., "Dynamic Properties of Lions' Gate Suspension Bridge," ASCE/EMD Specialty Conference on Dynamic Response of Structures: Instrumentation, Testing Methods and System Identification, University of California, Los Angeles, March 30 and 31, 1976.
3. Abdel-Ghaffar, A.M., "Dynamic Analyses of Suspension Bridge Structures", Earthquake Engineering Research Laboratory, EERL 76-01, California Institute of Technology, Pasadena, California, May 1976.
4. Abdel-Ghaffar, A.M. and Housner, G.W., "Vibrations in Suspension Bridges", Proceedings of Sixth World Conference on Earthquake Engineering, New Delhi, India, January 10-14, 1977, pp. 6-183 to 6-188.
5. Abdel-Ghaffar, A.M., "Vibration Studies and Tests of a Suspension Bridge", submitted to the International Journal of Earthquake Engineering and Structural Dynamics, January 1977.
6. Foutch, D.A., "A Study of the Vibrational Characteristics of Two Multistory Buildings", Earthquake Engineering Research Laboratory, EERL 76-03, California Institute of Technology, Pasadena, California, September 1976.
7. Okamoto, S. and Kubo, K., "Measurements of the Damping Coefficient of Suspension Bridges", Monthly Journal of the Institute of Industrial Science, University of Tokyo, Vol. 9, No. 12, 1957.
8. Kuribayashi, E. and Narita, N., "Vibration Test of the Wakato Suspension Bridge", 6th Symposium of Earthquake Engineering, Japan, 1963.
9. Report on "Earthquake Resistant Design for Civil Engineering Structures, Earth Structures and Foundations in Japan", Compiled by the Japan Society of Civil Engineers, 1977.

APPENDIX A

Fourier Amplitude Spectra of the Velocity Proportional Response  
of the Vertical and Lateral Motions Recorded at Stations 4 and 6  
and the Reference Station.

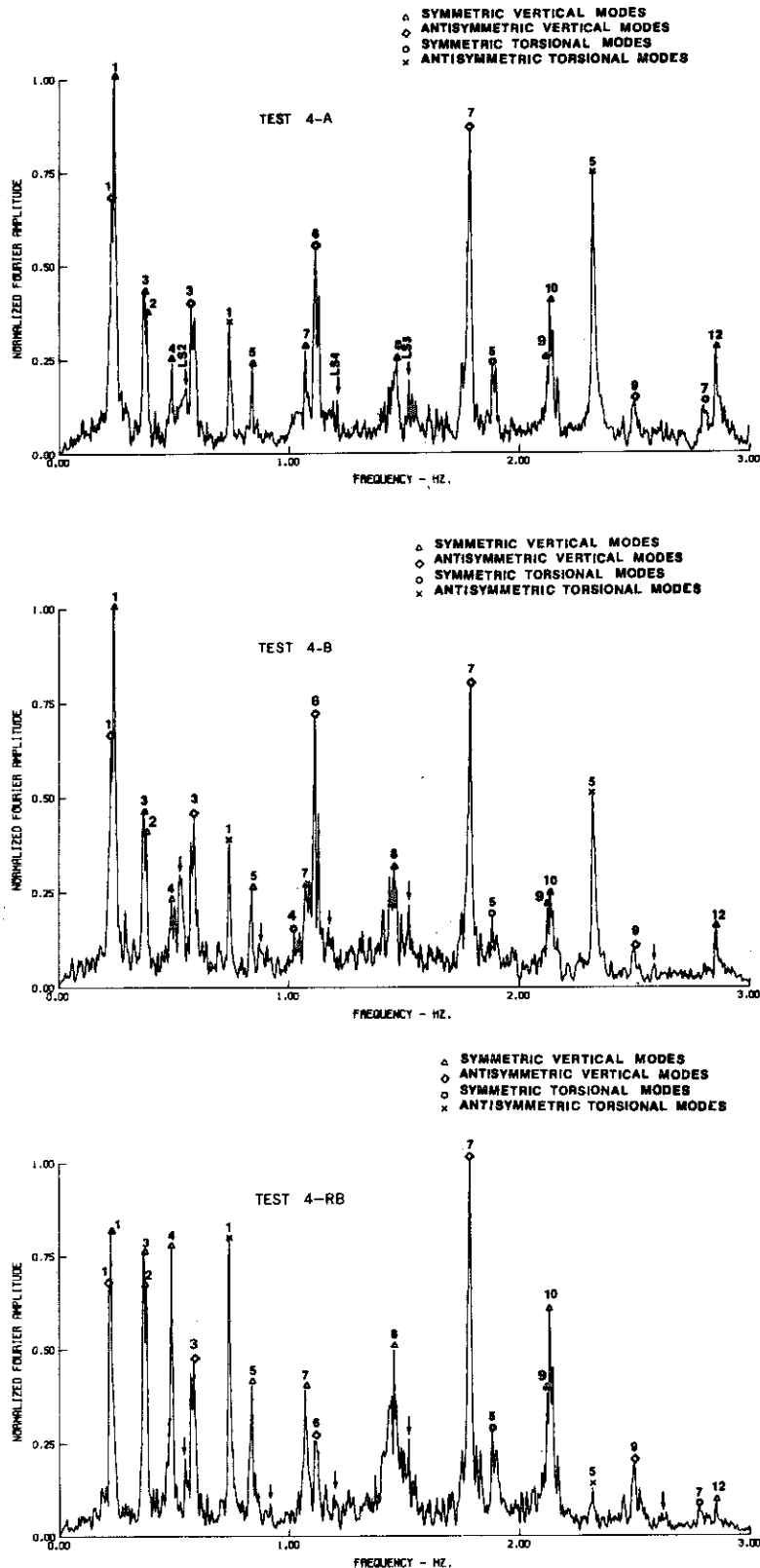


Fig. A-1. Fourier amplitude spectra of the velocity proportional response of the vertical motions recorded, simultaneously, at station 4 and the reference station.



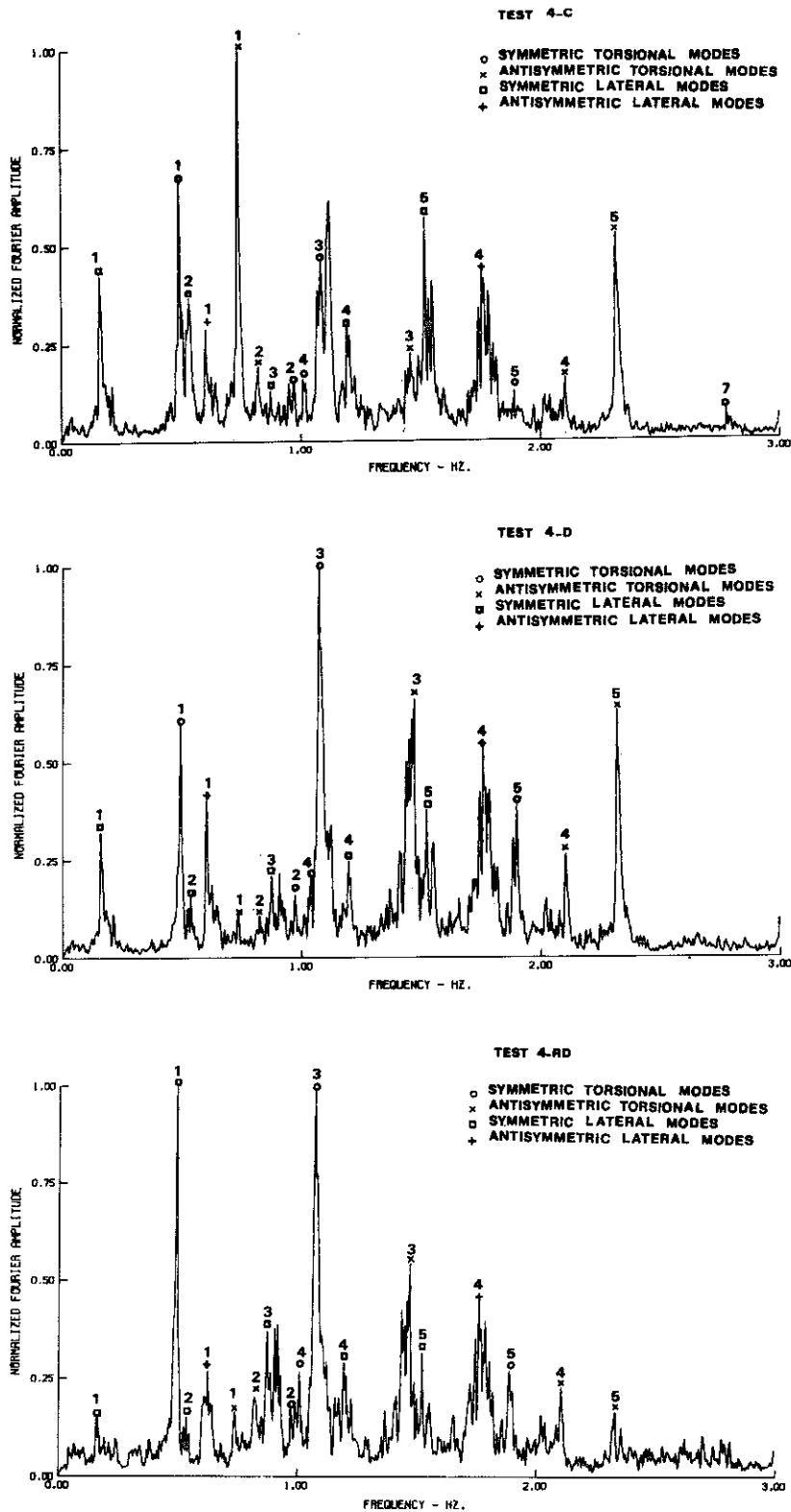


Fig. A-2. Fourier amplitude spectra of the velocity proportional response of the lateral motions recorded, simultaneously, at station 4 and the reference station.

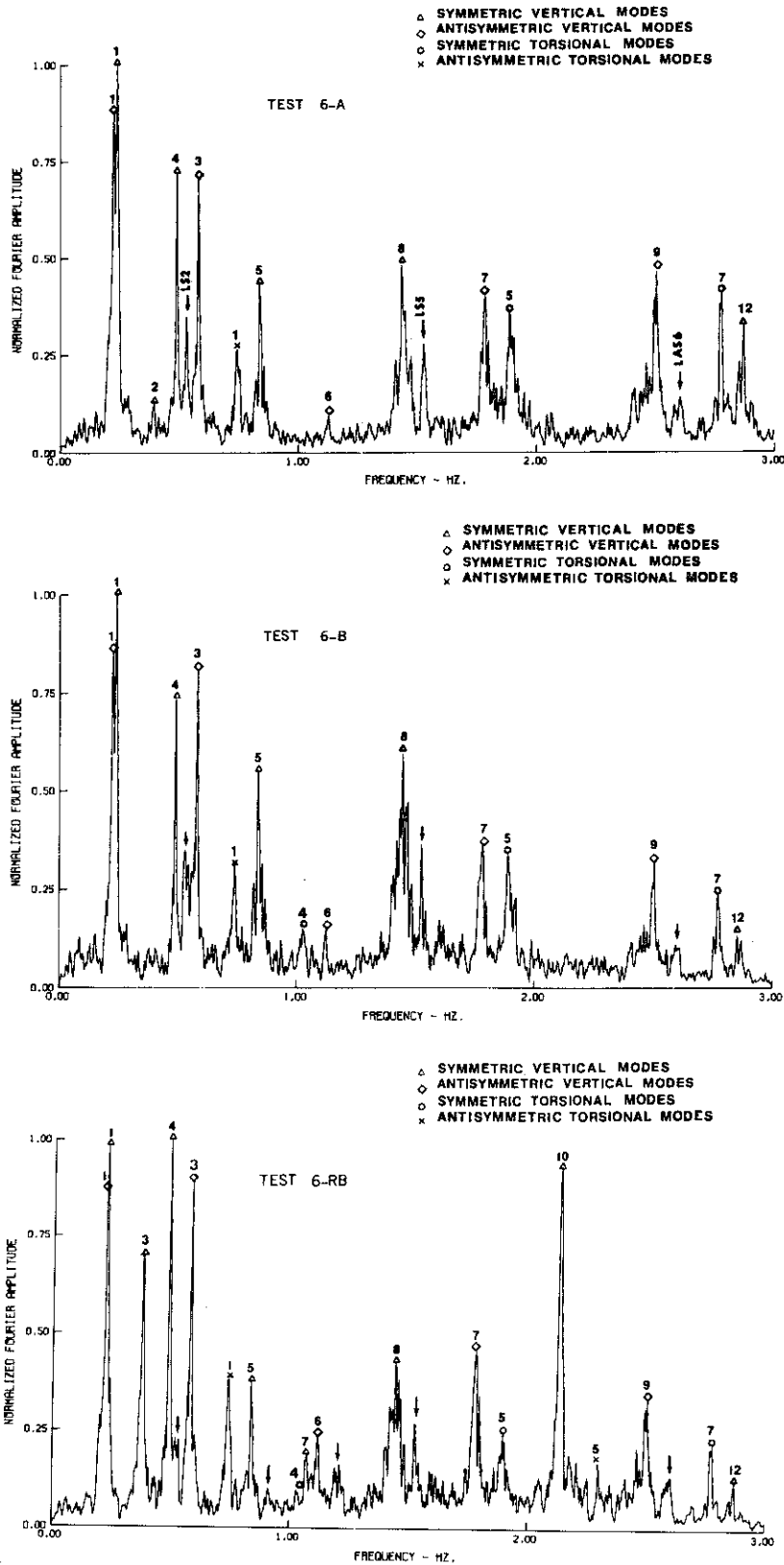


Fig. A-3. Fourier amplitude spectra of the velocity proportional response of the vertical motions recorded, simultaneously, at station 6 and the reference station.

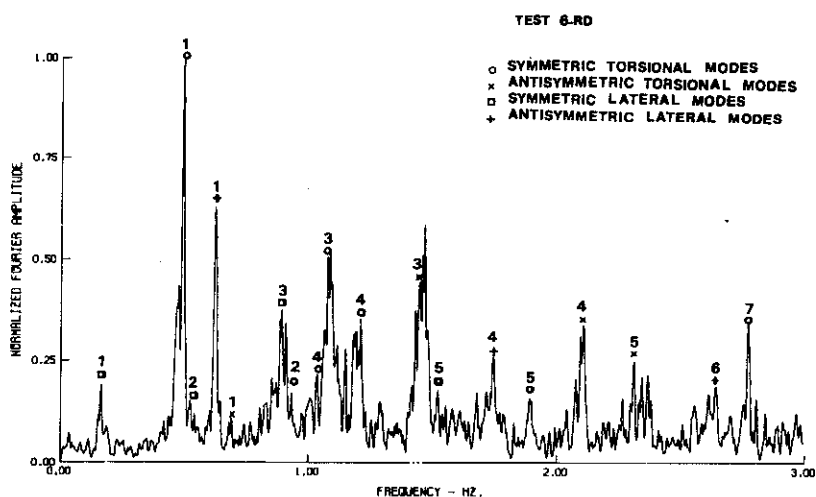
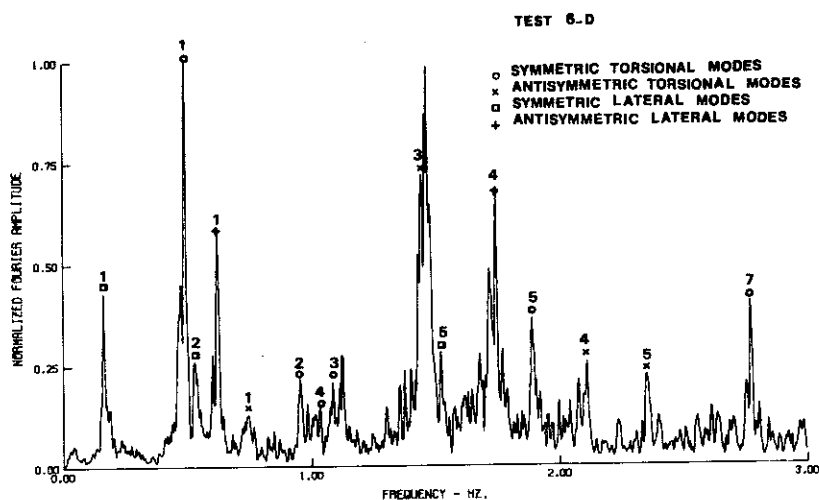
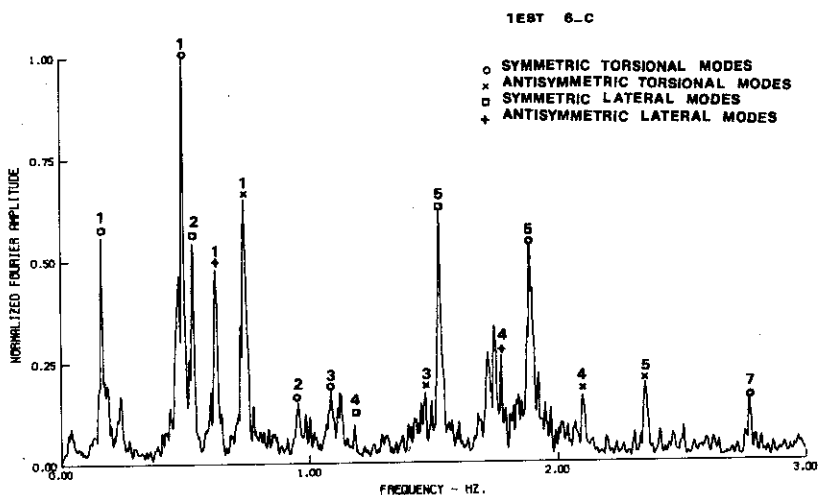


Fig. A-4. Fourier amplitude spectra of the velocity proportional response of the lateral motions recorded, simultaneously, at station 6 and the reference station.